Removal of *N*-Nitrosodimethylamine and other disinfection by-product precursors from tertiary wastewater effluent by activated carbon

by

Riley Edward Mulhern
B.S. Wheaton College, IL, 2014

A thesis submitted to the
Faculty of the Graduate School of the
University of Colorado in partial fulfillment
of the requirements for the degree of
Master of Science
Department of Civil, Environmental, and Architectural Engineering
2016

This thesis entitled:

Removal of *N*-Nitrosodimethylamine and other disinfection by-product precursors from tertiary wastewater effluent by activated carbon

written by Riley E. Mulhern

has been approved for the
Department of Civil, Environmental, and Architectural Engineering.

_____

R. Scott Summers, (Chair)

_____

JoAnn Silverstein

_____

Eric Dickenson

June 28, 2016

The final copy of this thesis has been examined by the signatories, and we find that both the content and the form meet acceptable presentation standards of scholarly work in the above-mentioned discipline.

ABSTRACT

Mulhern, Riley E. (M.S. Environmental Engineering)

Removal of *N*-Nitrosodimethylamine and other disinfection by-product precursors from tertiary wastewater effluent by activated carbon

Thesis directed by R. Scott Summers, Professor, Department of Civil, Environmental and Architectural Engineering, University of Colorado at Boulder

Organic constituents at the low to sub-microgram per liter level derived from wastewater effluents represent precursors to previously undetected disinfection by-products (DBPs) in drinking water utilities. *N*-nitrosodimethylamine (NDMA) is an emerging DBP of particular concern due to its suspected genotoxicity and carcinogenicity an order of magnitude greater than currently regulated DBPs. Granular activated carbon (GAC) has been shown to be a potential control technology for removing NDMA precursors from wastewater effluent, but adsorption behavior of specific precursor material is still poorly understood. The goal of this research is to expand knowledge of the GAC adsorption behavior of NDMA and other DBP precursors in wastewater effluent, including understanding the effect of different activated carbon types, the effect of varying GAC column Empty Bed Contact Time (EBCT), the effect of source water blending on NDMA precursor sorption, and the breakthrough of NDMA precursors relative to trihalomethane, haloacetic acid, and haloacetonitrile precursors. Lignite-based and wood-based activated carbon were found to remove NDMA precursors better than coconut-shell and bituminous carbons, presumably due to larger mesopore volumes. NDMA precursors are thought

to be larger molecular weight compounds or behave in water such that adsorption occurs in the mesopore region. A distinct non-adsorbable fraction in powdered activated carbon batch tests suggests a range of different precursor compounds. In Rapid Small-Scale Column Tests (RSSCTs), a simulated 20-minute bench-scale EBCT performed better than a 10-minute column, thus longer EBCTs are suggested when optimizing GAC control for NDMA precursors in wastewater. NDMA precursors were also found to adsorb independently of bulk organic matter and other DBP precursors, suggesting its precursors are distinct from currently regulated and other nitrogenous DBPs. As a result, Overall Fluorescence Intensity was proposed as a possible surrogate for NDMA precursors due to its similar adsorption behavior in RSSCTs using blended influent waters. Evidence is also presented for considering NDMA precursors as similar to micropollutants due to rapid sorption in batch testing distinct from DOM, and diminished impacts of influent concentrations on fractional RSSCT breakthrough.

Dedication

To the men and women of Telica, Nicaragua who inspired me to pursue this path;
and to Maggie who has walked it with me.

Acknowledgements

My solitary name on the cover of this thesis is a wild exaggeration. I could not have taken even two steps into the lab without the guidance and encouragement of my advisors, peers, and colleagues. This work represents the steepest learning curve I have ever had to climb, and I am grateful to everyone who has helped haul me up it. I am most humbled and surprised by the persistent, almost stubborn confidence Scott Summers had in me from day one. Even when I was sure that I was underqualified, ill prepared and generally making a mess of things, Scott looked me in the eye with remarkable patience and utter belief that I could and would succeed. In that, he gave me something valuable and lasting, and for which I am remarkably thankful.

Although, I probably still would *not* have succeeded if it were not for Dorothy Noble. It was Dorothy who helped me actualize the theory behind this work into experiments we could run; only with her help did I concretely accomplish anything. Together, we learned the difficulty of Formation Potential testing, she graciously pushed on ahead with me when I made mistakes, and became a constant support. Kyle Shimabuku and Leigh Gilmore were equally as important. Both Leigh and Kyle filled a mentoring role to me in all my lab work. This meant teaching me *everything:* where everything is, how to use every instrument, which buttons to push and which ones not to, how to grind carbon and pack columns… the list is endless. I am so fortunate to have entered into research at a time when I had such patient, willing, and knowledgeable support from my peers. Nathan Yang was also a very real encouragement and practical help at many critical and stressful times, and I certainly could not have done anything meaningful with fluorescence were it not for Garrett McKay. I will miss the friendships and camaraderie of working together with all my fellow lab mates.

Thanks are also owed to the Water Research Foundation for funding this work. Eric Dickenson, Detlef Knappe, Caitlin Glover, and Amy Cuthbertson on the Water Research Foundation project team also played important roles in developing this data, including a remarkable effort of logistics shipping samples across the country. I am grateful to have been a part of such a capable and supportive team.

Finally, although some of my family could not quite remember what I was studying these past two years—"How are those *chlorimites*?"—they were perhaps the most important in getting me to this point. I have been blessed to have my Mom, Dad, Mother and Father-in-Law all nearby during this season to selflessly care for and encourage me. And Maggie, you have accompanied me more closely than anyone through every step of this work by your constant love. Thank you.

TABLE OF CONTENTS

LIST OF TABLES

LIST OF FIGURES

CHAPTER 1: INTRODUCTION

1.1 Motivation

The combined effects of widespread disinfection of drinking water and wastewater treatment profoundly improved public and environmental health in the United States during the 20th century. Prior to the implementation of chlorine in drinking water and the development of wastewater treatment technologies, fecal pathogens were pervasive in the environment and waterborne disease was epidemic. Implementing clean water technologies led to vast reductions in nationwide mortality rates and drinking water contamination (Adler et al., 1993; Cutler and Miller, 2005).

However, unintended chemical hazards have emerged from the compounding effects of these treatment processes. The introduction of chemical disinfection was found to also result in the formation of toxic disinfection by-products (DBPs) as a result of reactions with natural organic matter (NOM), having the potential to cause cancer and birth defects (Richardson et al., 2007; Villanueva et al., 2004; Waller et al., 1998). Additionally, treated wastewater effluents are being identified as large contributors of trace organic contaminants in natural waters (Kolpin et al., 2002), which represent new and potentially more harmful DBP precursors in municipal water supplies, especially as population growth and water scarcity cause increasing de facto wastewater reuse (Krasner et al., 2008; Rice et al., 2013). Indeed, many drinking water utilities in the United States rely on source waters with greater than 90 percent wastewater influence during dry periods of the year (Rice, Wutich, and Westerhoff 2013).

Thus the growing number of precursors in drinking water influent warrants increasing public health concern regarding DBPs in the United States. *N*-nitrosodimethylamine (NDMA) is a currently unregulated DBP of particular concern due to its suspected genotoxicity and carcinogenicity an order of magnitude greater than currently regulated DBPs (USEPA, 2002). As a priority contaminant, the EPA has set an exceedingly low lifetime NDMA exposure limit of 0.7 ng/L for a 10^{-6} increased cancer risk, while the State of California has issued a Public Health Goal of 3 ng/L in drinking water (Cal/EPA, 2006; USEPA, 2002). NDMA has previously been known as a contaminant in certain consumer products and in groundwater from industrial uses (ATSDR, 1989; HSDB, 2013) but has only recently been identified as a DBP (William A Mitch et al., 2003). Much attention has been paid to high concentrations of NDMA precursors in effluent organic matter (EfOM) from the compounding contributions of sewage, polymeric coagulant aids, and pharmaceuticals and personal care products (PPCPs) (Krasner et al., 2013, 2008; Le Roux et al., 2011; Shen and Andrews, 2011, 2013).

High NDMA formation has also been correlated with the use of chloramines instead of chlorine for disinfection (Woods and Dickenson, 2015) and thus warrants additional concern due to the increased practice of chloramination in drinking water utilities since the implementation of the USEPA Stage 2 DBP Rule (Li, 2011). A formation pathway has been identified in the reaction of dimethylamine with monochloramine (Choi and Valentine, 2002; Mitch and Sedlak, 2002). However, the low yields from this reaction suggest that NDMA formation cannot be accounted for by DMA alone and it is thus likely that NDMA precursors are diverse in properties and origins (William A. Mitch et al., 2003).

Concentrations of currently regulated DBPs—trihalomethanes (THMs) and haloacetic acids (HAAs)—are generally used as indicators for levels of other DBPs in drinking water from

the use of both chlorine and chloramines. However, as a result of the various and complex precursors in EfOM distinct from NOM, very little is known regarding overall DBP formation in wastewater from chlorine/chloramines relative to regulated DBPs, especially as it relates to NDMA.

Even less is known regarding control of chlorinated/chloraminated DBP precursors in EfOM. Current research focuses on strategies for removing the precursor material responsible for emerging DBP formation, rather than introducing alternative disinfectants or additional layers of treatment after formation. The use of granular activated carbon (GAC) for the removal of regulated chlorinated and chloraminated DBP precursors in drinking water has been studied in depth and is well understood (Summers et al., 2010). Knowledge gaps still exist, however, in the utility of GAC for removing regulated and unregulated DBP precursors from EfOM.

Under chloramination conditions, Hanigan et. al. (2012) have reported GAC to be a potential control technology for wastewater-derived NDMA precursors, but the effect of changing operational parameters such as GAC type and Empty Bed Contact Time (EBCT) have not been considered. Furthermore, given evidence that traditional indicators of organic matter used to track regulated carbonaceous DBP precursor removal poorly describe nitrogenous NDMA precursor removal in GAC columns, a better surrogate is necessary for monitoring adsorption of NDMA precursors by GAC in waters with varying wastewater content. Finally, the adsorption behavior of chloraminated NDMA precursors relative to specific other chlorinated/ chloraminated DBP precursors has not been evaluated previously and represents an important gap in understanding for mitigating the public health impacts of wastewater reuse.

1.2 Research Objectives

This goal of this thesis is to increase the limited understanding of the complex adsorption behavior of chlorinated and chloraminated DBP precursors in the presence of EfOM, in order to better assess the feasibility of using GAC to control NDMA formation in wastewater-impacted waters. Thus the objectives of this study are:

1. Evaluate the impact of chlorine and chloramine disinfection on the formation of regulated and unregulated DBPs in wastewater effluent
2. Evaluate the effectiveness of different GAC types in removing NDMA precursors in wastewater effluent
3. Evaluate the effect of EBCT on wastewater-derived DBP precursor removal under chlorination and chloramination conditions
4. Quantify the breakthrough of NDMA precursors relative to regulated DBP precursors and bulk organic matter breakthrough
5. Evaluate the effect of influent blending on adsorption behavior of wastewater-derived DBP precursors in GAC columns

1.3 Research Approach

The objectives of this study will be accomplished using bench-scale experiments as a tool to rapidly evaluate the effectiveness and feasibility of GAC in controlling EfOM precursors. Tertiary wastewater effluent from partner utility Clark County Water Reclamation District (CCWRD) in Las Vegas, Nevada will be utilized in powdered activated carbon (PAC) batch tests and Rapid Small-Scale Columns Tests (RSSCTs). Formation Potential (FP) testing will be used to evaluate the removal of precursors in GAC experiments, in lieu of specific precursor

identification since precursors are non-homogenous. Both chlorine and chloramines will be used to form DBPs before and after GAC treatment to evaluate potential precursor preferences between disinfectant types and differences in precursor sorption behavior. Finally, CCWRD wastewater will be blended with a non-wastewater impacted, coagulated drinking water to observe the effects of blending on NDMA and other EfOM DBP precursor removal in bench-scale GAC columns. This data will provide an important basis for future research on scale-up of RSSCT results to pilot and full-scale GAC columns.

CHAPTER 2: MATERIALS AND METHODS

2.1 Analytical Methods

Total organic carbon (TOC) was measured using a Sievers 800 TOC Analyzer (Sievers Instruments Inc., CO) in accordance with Standard Method 5310C (APHA, 2005). Ultraviolet absorbance (UVA) was analyzed at a wavelength of 254 nm using a HACH DR4000 Spectrophotometer (HACH, CO) in accordance with Standard Method 5910 (APHA, 2005).

Fluorescence spectroscopy was performed using a FluoroMax-4 spectrofluorometer (JohnYvon Horiba, NJ). Excitation and emission profiles (EEMs) were collected by measuring emission scans between 300 nm and 560 nm (at 2 nm increments), at excitation wavelengths every 10 nm between 250 nm and 450 nm. A 5 nm bandpass and 0.25 second integration time were used. EEMs were then corrected and analyzed using MATLAB software (Mathworks, MA) in accordance with methods outlined by Korak et al. (2014). Inner filter corrections were made with a UV-Vis absorbance scan collected using a Cary-100 Spectrophotometer (Agilent Technologies, CA). Ultrapure 18.2 MΩ-cm blanks, Raman peaks, and lamp scans were collected before each fluorescence analysis and used during correction analysis and as instrument quality control measures. Peak intensities were then calculated using an algorithm-based approach to select the maximum intensity within specified excitation emission regions. Peaks in the A and C regions are more characteristic of humic-like organic matter, while peaks in the B and T regions are representative of more protein-like/nitrogen containing compounds (Julie A Korak et al., 2014; Julie A. Korak et al., 2014). Overall fluorescence index (OFI), was calculated by summing the intensities of the entire EEM in Raman Units (RU) (Beggs et al., 2009). Fluorescence Index

(FI) is calculated as the ratio of the emission intensity at 470 nm over the intensity at 520 nm at an excitation wavelength 370 nm, according to the method originally developed by McKnight et al. (2001) and later adjusted by Cory et al. (2010).

Influent nitrate/nitrite concentrations were measured at the Southern Nevada Water Authority (SNWA) using colorimetric analysis according to EPA Methods 353.2. Ammonia was measured by spectrophotometry by Standard Method 4500-G and total nitrogen (TN) was measured using a Shimadzu Total Nitrogen Module (Shimadzu Scientific Instruments, Inc., MD), also at SNWA. NDMA analysis was performed at SNWA using automated solid-phase extraction and GC-MS/MS analysis, adapted from EPA Method 521 (Holady et al., 2012). The analytical relative standard deviation (RSD) in tertiary wastewater (n=6) is reported to be 7 percent (Holady et al., 2012). Total trihalomethane (TTHM), haloacetic acid (HAA8), and haloacetonitrile (HAN) analysis was performed according to EPA Methods 551.1 and 552.2 using gas chromatography (6890 GC, Agilent Technologies, CA) at the University of Colorado Boulder. HAA8 data is reported instead of HAA9 because the instrumentation used was unable to distinguish tribromoacetic acid from baseline values. Emerging DBP analysis (including Total Nitrogenous, Brominated, Iodinated, and Chlorinated DBPs) was carried out using liquid-liquid extraction techniques at the University of South Carolina. A complete listing of the emerging DBP analytes tested for can be found in Appendix A1. Methods utilized were developed at the University of South Carolina and are not yet published. Further detail into the sampling and extraction procedure for emerging DBPs is provided in Appendix A2.

2.2 Waters

Wastewater effluent used in batch testing and RSSCTs was received at the University of Colorado Boulder from Clark County Water Reclamation District (CCWRD) in Las Vegas, Nevada. Tertiary treated wastewater effluent, optimized for biological phosphate removal, was collected after dual-media filtration prior to ultraviolet (UV) disinfection. Three separate batches of CCWRD wastewater were used over the course of this study. WW1 was used in batch testing experiments. WW2 was used in preliminary RSSCTs to test the effect of EBCT. WW3 was used along with a drinking water (DW1) in testing the effect of blending RSSCTs. DW1 was taken from Betasso Water Treatment Plant in Boulder, Colorado. Betasso Water Treatment Plant draws from a non-wastewater impacted source water, Boulder Creek, and water was collected after alum coagulation. DW1 was spiked with bromide to match the bromide levels present in WW3 so that bromide concentration of blended waters would stay constant, and brominated DBP formation could be more accurately compared across RSSCTs. Bromide concentrations and additional influent parameters for each batch of water are summarized in Table 2.1.

The three batches of wastewater effluent showed consistent organic matter characterizations, with TOC in the narrow range of 5.76 to 6.10 mg/L, and UVA between 0.102 and 0.111 cm^{-1} over the course of eight months. OFI was also consistently between 1400 and 1500 R.U. in each batch of wastewater. The fluorescence index (FI) was high in all three wastewater batches (>2) while SUVA values were low (<2 L/mg/m), indicating relatively low hydrophobicity and aromaticity, typical of wastewater effluent organic matter (EfOM) (Ma et al., 2001; Pernet-coudrier et al., 2008). However, fluorescence EEMs did not show strong signatures in the B and T regions relative to A and C, and no distinct peaks in the B and T ranges at all, as can be seen in Figure 2.1 for WW2. WW1 and WW3 showed similar fluorescence spectra. This

reveals that there is still a meaningful aromatic, humic-like component in the influent wastewater and that protein-like microbial products are not a dominant component of EfOM used in this study. It should be noted that this is unique from previous research which has shown other wastewater effluents to exhibit stronger fluorescence intensities in the protein-like regions than humic regions (Krasner et al., 2008).

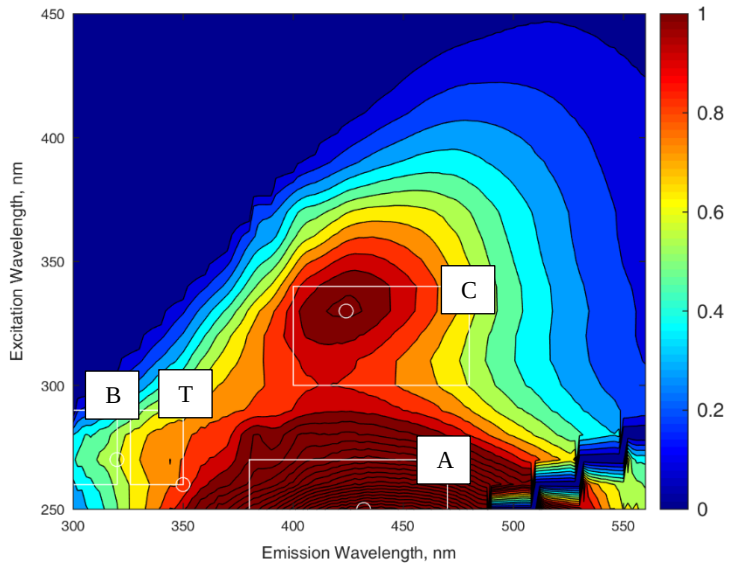

Figure 2.1: Excitation emission matrix for WW2. Intensities are given in Raman Units (R.U.) Boxes outline the four regions, where A and C are humic-like and B and T and protein-like compounds. Hollow circles show location of peak intensity in each region.

DW1 had very low DOM content, with a TOC of 1.02 mg/L, UVA of 0.018 cm^{-1}, and OFI of 80 R.U. SUVA values in DW1 were also low, similar to the wastewater effluent, due to the effects of coagulation (Bell-Ajy et al., 2000). FI was lower than the wastewater, which could indicate smaller size of the influent organic matter in DW1 (Mostafa et al., 2014).

Nitrogen speciation was dominated by nitrate in all three wastewater effluents according to data collected from a 12-month history. Nitrite and ammonia were below detection limits. The 12-month mean for total nitrogen (TN) was slightly below the 12-month mean for nitrate, but

this can be accounted for by the different method of measurement used for the two parameters (see 2.1 Analytical Methods). Overall, the mean TN concentration was within one standard deviation of mean nitrate concentrations, revealing that almost all the nitrogen present is in the form of nitrate, and that dissolved organic nitrogen (DON) concentrations are also low. Nitrogen speciation data was not collected for DW1. Influent DBP concentrations were also extremely low, and background NDMA was undetectable in any of the waters used in this study.

Table 2.1: Bench-scale influent water quality parameters, ± 1 standard deviation from duplicate measurements.

Batch	**WW1**	**WW2**	**WW3**	**DW1**
Date	Jun-Aug 2015	Oct-Nov 2015	Dec-Feb 2016	Dec-Feb 2016
pH	7-8	7-8	7-8	7-8
TOC (mg/L)	5.76 ± 0.19	5.28 ± 0.74	6.10 ± 0.24	1.02 ± 0.1
UVA (cm^{-1})	0.103 ± 0.001	0.102 ± 0.01	0.111 ± 0.003	0.018 ± 0.005
SUVA (L/mg/m)	1.78 ± 0.05	1.93 ± 0.15	1.82 ± 0.07	1.78 ± 0.47
OFI (R.U.)	1474	1435	1438	80
Fluorescence Index	2.03	2.03	2.07	1.66
Bromide	153 ± 16*	153 ± 16*	162	166†
Nitrate (mg/L as N)*	11.3 ± 0.8	11.3 ± 0.8	11.3 ± 0.8	-
Nitrite (mg/L as N)*	<0.020	<0.020	<0.020	-
Ammonia (mg/L as N)*	<0.020	<0.020	<0.020	-
Total N (mg/L)*	10.8 ± 0.8	10.8 ± 0.8	10.8 ± 0.8	-
NDMA (ng/L)	<2.5	<2.5	<2.5	<2.5
TTHMs (μg/L)	1.06	0.00	0.00	0.00
HAA5s (μg/L)	1.92	2.91	0.291	0.00
HAA8s (μg/L)	1.92	3.57	0.952	0.630
HANs (μg/L)	0.129	0.142	0.147	0.00

*Average from 12-month history
†After bromide spike

2.3 Disinfection

Two disinfectants were used in this study at two different doses. Monochloramine (NH_2Cl) and Sodium Hypochlorite (NaOCl) were tested using both Formation Potential (FP) and Uniform Formation Conditions (UFC) procedures. UFC tests were only performed on influent

waters in order to have a baseline comparison of DBP formation between FP and UFC procedures. FP tests were chosen as the preferred method to track precursor removal after activated carbon treatment to ensure that all DBPs were formed. This was especially important when tracing NDMA precursors which were found to exist in wastewater effluent at exceedingly low levels. All reagents used were certified ACS grade, supplied from Fisher Scientific. Only amber glassware was used for FP and UFC testing. All glassware was triple-rinsed with 18.2 MΩ-cm ultrapure water, heated to 550 degrees Celsius for 3 hours, and cooled before use.

2.3.1 Formation Potential Tests

Monochloramine. Fresh NH_2Cl solution was prepared before each use by dissolving Ammonium Chloride in refrigerated, ultrapure 18.2 MΩ-cm water adjusted to pH 9 with Sodium Hydroxide pellets. Laboratory grade NaOCl (5.65-6% w/v) was added to achieve a concentration of 1.4 g/L total chlorine as Cl_2. Concentration was verified before dosing using the colorimetric N,N Diethyl-1,4 Phenylenediamine Sulfate (DPD) method for total chlorine. NH_2Cl solution was used immediately. Samples were then spiked with monochloramine to achieve 140 mg/L total chlorine as Cl_2. One percent of the sample volume was also spiked with phosphate buffer prepared with equal parts mono- and di-basic sodium phosphates and adjusted to pH 7. Influent and batch test waters were filtered through a 1.2 µm glass filter before dosing. RSSCT effluents were not filtered since the carbon bed as well as glass pre- and post-filters effectively removed particulate matter. NDMA samples retained less than 10 percent headspace, while all other DBP samples were filled to no headspace. Samples were stored in the dark at room temperature for 10 days and tested using DPD for a remaining total chlorine residual of approximately 10 mg/L or higher. NDMA samples were then quenched with 80 mg/L Sodium Thiosulfate and 1 g/L

Sodium Azide before shipment to SNWA for NDMA analysis. THM, HAA, and HAN samples were poured off into 60 mL vials quenched with 7-8 mg of Sodium Thiosulfate per vial, according to procedures outlined by EPA Method 524.2 and analyzed at CU Boulder. The method RSD for NDMA FP (n=3) was approximately 2 percent. The average method RSD for chloraminated TTHMs, HAA8s, and HANs from duplicates on multiple waters (WW1 and WW2) was less than 20 percent. Emerging DBP samples were quenched by dropping the pH to 3.5-4 with H_2SO4 and with approximately 32 mg/L Ascorbic Acid before being shipped to the University of South Carolina for analysis.

Chlorine. Standard chlorine solution was prepared in advance by diluting NaOCl solution in ultrapure 18.2 MΩ-cm water and mixing with 1 molar Borate buffer to achieve an initial 0.077 molar NaOCl solution. Chlorine concentration was tested each day before use via the free chlorine DPD method and the solution was remade if the concentration dropped below 4000 mg/L as Cl_2. All samples were dosed at one-percent volume by volume using the standard chlorine solution with no headspace. Samples were stored in the dark at room temperature for 10 days to yield free chlorine residuals of approximately 50 mg/L as Cl_2. All samples were poured off into 60 mL vials quenched with 6-7 mg of Ammonium Chloride according to EPA Method 551.1 procedures, and analyzed at CU Boulder. The average method RSD for chlorinated TTHMs, HAA8s, and HANs from duplicates on multiple waters (WW1 and WW2) was less than 10 percent.

2.3.2 Uniform Formation Conditions Tests

UFC procedures were adapted from Summers et al. (1996). A three-day UFC test was considered in order to be representative of average maximum conditions in the distribution

system. Monochloramine and chlorine solutions were prepared as outlined above. A three-day demand study was performed on each water for which a full UFC test was performed. Three 125 mL bottles of sample were spiked at three different doses based on different Cl_2:TOC ratios, and filled with no headspace. Residuals were read after three days and plotted according Cl_2:TOC ratios. Linear regression analysis was performed to predict the dose to yield a residual of approximately 1 mg/L after three days. Samples were then dosed according to this analysis, using the same procedure for chlorine and monochloramine. After three days, residuals were read with an acceptable range of 0.6-1.4 mg/L (Summers et al., 1996). UFC NDMA samples were then poured off into 1 liter bottles quenched with 80 mg/L Sodium Thiosulfate and 1 g/L Sodium Azide and shipped to SNWA. All other UFC DBP samples were poured off into 60 mL vials quenched with either Ammonium Chloride or Sodium Thiosulfate (see above), depending on whether monochloramine or chlorine was used. DBP samples other than NDMA were analyzed at CU Boulder.

2.4 Adsorbents

The adsorbents used in this study and their general properties are summarized in Table 2.2. Mezzari (2006) performed in-depth characterizations of each of the adsorbents used in this study. Four different feed materials were tested, including thermally activated coconut-shell based GAC (AquaCarb 1230C, Evoqua Water Technologies, Warrendale, PA), thermally activated bituminous-based GAC (F400, Calgon Corporation,) thermally activated lignite-based GAC (Hydrodarco 3000, Cabot Norit Corporation, Boston, MA), and chemically activated wood-based GAC (Picazine, PicaUSA, Columbus, OH). Batch tests utilized all four GAC types, while RSSCTs used HD3000 only. GACs were ground using mortar and pestle and particle sizes

isolated using US Standard sieves on a sieve shaker table. For batch testing, carbons were ground to PAC size by passing through a #325 sieve (particle diameter ≤ 0.044 mm), then dried at 100 degrees Celsius for 24 hours, and stored in a capped glass vial in a desiccator before use. For RSSCTs, the fraction between #100 and #200 sieves (log mean particle diameter of 0.11 mm) was collected, then rinsed and decanted iteratively in 18.2 MΩ-cm water to remove particle fines. Remaining in ultrapure water, GAC was then degassed in a vacuum for 24 hours and stored in a capped bottle until use.

Table 2.2: Activated carbon properties used in batch testing and RSSCTs.

	AC1230C	**F400**	**HD3000**	**Picazine**
Producer:	Evoqua	Calgon	Cabot-Norit	PICA-USA
Feed Material:	Coconut-shell	Bituminous coal	Lignite coal	Wood
Activation:	Thermal	Thermal	Thermal	Chemical
Mesh size:	12x30	12x40	8x30	approx. 8x25[†]
Apparent Density (g/cm^3):	0.46-0.52	0.54	0.38	0.45[†]
BET Surface Area (m^2/g):	1157	932	525[a]	1460[†]-1680*
Micropore Volume (cm^3/g):	$4.37x10^{-1}$	$3.35x10^{-1}$	$1.48x10^{-1}$ [a]	$4.96x10^{-1}$
DFT Mesopore Volume (cm^3/g)[b]:	$4.37x10^{-1}$	$1.34x10^{-1}$	$4.56x10^{-1}$ [a]	$5.62x10^{-1}$

Apparent densities taken from producer data sheets unless noted
All surface area and pore volume data from Mezzari (2006) unless noted
* Li, Quinlivan, and Knappe (2005)
[†] Buczek (2016)
[a] Values given for Cabot-Norit HD4000, identical to HD3000 except 10x30 mesh full-scale size
[b] DFT Mesopore volume measured for pores with widths from 20 to 360 Å

2.5 Batch Tests

Using the PAC-size ground carbons, initial batch testing was performed on WW1 with each carbon type at doses of 5, 10 and 50 mg/L of PAC. Batch volumes of 4 liters were used in

order to have enough sample for FP testing using both chlorine and monochloramine. PAC was dosed and bottles were placed on a shaker table for 24 hours. Samples were then filtered through a 1.2 µm glass filter and spiked under FP conditions. Additional doses of 1.25 and 2.5 mg/L were tested on WW1 using HD300 once it was determined that it effectively removed NDMA precursors at the 5 mg/L dose. The method RSD for TOC based on duplicate measurements at the 5 mg/L dose across all carbons was approximately 5 percent. The method RSD for NDMA FP based on duplicate trials using HD3000 at the 5 mg/L dose was determined to be approximately 23 percent.

2.6 Rapid Small-Scale Columns Tests

RSSCTs were designed using the proportional diffusivity (PD) method originally developed by Crittenden and Berrigan (1987) which assumes that intraparticle diffusivity is proportional to particle size. Design parameters are presented in Table 2.3. This approach was chosen because PD-RSSCTs have been shown to yield better scale-up results for the removal of DOM (Crittenden et al., 1991). Thus, in order to test simulated EBCTs of 10 minutes and 20 minutes in this study, bench PD-RSSCT operation times were scaled according to particle diameter using the equation,

$$\frac{EBCT_{SC}}{EBCT_{LC}} = \frac{d_{p,SC}}{d_{p,LC}} = \frac{t_{SC}}{t_{LC}} \quad (1)$$

where the subscripts *SC* and *LC* refer to the small column and large column, respectively, d_p is particle diameter, and *t* is time of operation. Using HD3000 (8x30 mesh full-scale size) and 100x200 RSSCT particle size results in the design parameters summarized in Table 2.3 for

simulated 10- and 20-minute EBCTs. Using this approach, the 100x200 ground, decanted, and degassed carbon was loaded into 4.76 mm inside diameter Teflon columns at different bed lengths for the 10- and 20-minute columns (10- and 20-minute columns were run in parallel, not in series). Loading of the GAC was accomplished by filling the column with deionized water and using a glass dropper to pack the column while keeping the GAC particles completely submerged, so as to prevent reaeration of the pore volume. A glass wool post-filter supported the carbon at the bottom of the column.

Before start-up, the system was cleaned by recirculating deionized water with approximately 10 mg/L free chlorine for 24 hours. System flow rate was calibrated to 2.0 mL/minute during this time, and checked and adjusted daily after the start of the experiment. A Cole-Parmer Masterflex 7521-40 pump driver and 7090-62 Teflon diaphragm pump head circulated water through the system. A pulse dampener normalized the pulsing flow from the pump head and a glass wool pre-filter was installed to remove grit and particles in the wastewater than could lead to headloss in the column. After recirculation using the chlorinated influent, fresh deionized water was placed in the influent tank and the system was rinsed until no chlorine residual was detected in the effluent. The packed GAC column was then connected and run on deionized water until all air bubbles were removed. Deionized water was then replaced with the experiment influent water, held in a 20 Liter carboy, and pumped through the system until influent port above the GAC column. When the UVA measured at the influent port matched that of the influent tank the experiment was begun.

Effluent was collected as composite samples every 2-4 hours during the first 12 hours, then approximately every 24 hours thereafter. The volume of water in each composite effluent sample point was measured and used to calculate approximate total and average throughput (in

bed volumes) for each sample point. Each daily sample point was also tested for TOC and UVA in order to ensure proper column operation. Composite effluents were then refrigerated and stored in amber glass bottles until select effluent points were chosen for FP testing. The influent tank was replenished every 3-4 days, and influent samples were periodically taken from the influent tank and directly above the column. Columns were run for approximately three to four weeks.

For blended RSSCT influents, WW3 and DW1 were blended at ratios of 60 percent WW3 to 40 percent DW1, and 20 percent WW3 to 80 percent DW1, in order to represent a range of influent conditions drinking water utilities might face. 20 Liters of each ratio were blended at a time when the influent tank was low, rather than blending a large volume in advance. This was done to conserve the amount of water available for each end-member RSSCT (i.e., columns run using 100 percent WW3 and 100 percent DW1).

Duplicate RSSCT trials on 100 percent wastewater effluent using WW2 and WW3 resulted in robust reproducibility of the method with an average RSD value of 3 percent for TOC when comparing BV_{20} and BV_{50} values between runs. This result corresponds well with RSSCT method reproducibility demonstrated for TOC in previous work (Summers et al., 1995). NDMA FP showed greater variation between wastewater runs with an average RSD value of 18 percent. This wider range of reproducibility for NDMA FP is expected due to additional random error contributions from FP testing and NDMA analysis as well as greater variability of influent NDMA precursor concentrations than TOC. This amount of error would very likely be reduced if duplicate RSSCT trials were performed on the same batch of wastewater effluent, thus this represents a conservative estimation of the error.

Table 2.3: RSSCT column properties for simulated 10- and 20-minute EBCTs

	10-minute column	**20-minute column**
Carbon used:	HD3000	HD3000
$EBCT_{LC}$ (min):	10	20
$EBCT_{SC}$ (min):	0.84	1.68
Small column bed length (cm):	9.45	18.91
$d_{p,LC}$ (mm):	1.29 (8x30 mesh)	
$d_{p,SC}$ (mm):	0.11 (100x200 mesh)	
Scaling factor:	11.88	
Small column aspect ratio:	44	
Small column flow rate (mL/min):	2.00	
Small column hydraulic loading rate (m/hr):	6.74	
Small column Reynolds number:	0.6	

CHAPTER 3: RESULTS AND DISCUSSION

3.1 DBP formation before GAC treatment

In order to understand the DBP formation of wastewater-derived precursors, influent waters used in the study were exposed to monochloramine and free chlorine at FP and UFC doses. The DBP formation concentration and yield (DBP concentration normalized to TOC concentration) for each of the influent waters used in this study are summarized in Table 3.1. Formation results for batch WW2 are shown in Figure 3.1. Systematic differences in DBP formation were seen when each water was exposed to monochloramine and free chlorine under FP and UFC dose conditions. Wastewater effluent and drinking water batches also showed distinct formation results.

Table 3.1: Comparison of raw water DOM and DBP formation values for different batches under FP and UFC conditions using monochloramine and free chlorine. Concentrations in µg/L, yields in µg/mg, ± 1 standard deviation from duplicate trials.

Batch	**WW1**	**WW2**	**WW3**	**DW1**
Monochloramine FP				
NDMA	**0.960**	**0.590**	**0.747 ± 0.012**	**0.017**
yield	0.17	0.11	0.13 ± 0.03	0.0167
TTHMs	**29.1 ± 3.7**	**33.4 ± 3.2**	**63.4**	**23.3**
yield	5.1 ± 0.5	6.2 ± 0.5	11.0	22.5
HAA5s	**47 ± 12.5**	**40 ± 0.2**	**85.0**	**19.8**
yield	8.2 ± 2.4	7.53 ± 0.1	14.7	19.4
HAA8s	**60.3 ± 19**	**48.2 ± 0.13**	**93.9**	**24.1**
yield	10.6 ± 3.7	9.0 ± 0.1	16.3	23.5
HANs	**7.9 ± 2.7**	**7.07 ± 0.38**	**14.3**	**3.16**
yield	1.4 ± 0.5	1.3 ± 0.1	2.5	3.1
Total Cl-DBPs	-	-	**185 ± 4.8**	**39.7 ± 4.7**
yield			30.3	38.9

Total I-DBPs		-	-	**5.7 ± 0.2**	**NA**
	yield			0.9	NA
Total Br-DBPs		-	-	**39.5 ± 2.0**	**32.8 ± 4.3**
	yield			6.5	32.2
Total N-DBPs		-	-	**114 ± 16**	**30.7 ± 4.7**
	yield			18.7	30.1
Free chlorine FP					
TTHMs		**739 ± 63**	**686 ± 14**	-	-
	yield	128 ± 7.6	128 ± 0.7		
HAA5s		**489 ± 3.7**	**454**	-	-
	yield	85 ± 2.9	86		
HAA8s		**625 ± 23**	**577**	-	-
	yield	109 ± 6.8	109		
HANs		**0.28**	**0.128 ± 0.003**	-	-
	yield	0.05	0.02 ± 0.0001		
Monochloramine UFC					
NDMA		**0.260**	**0.420**	-	-
	yield	0.046	0.079		
TTHMs		**9.7**	**2.7**	**3.8**	**4.2**
	yield	1.7	0.5	0.6	4.1
HAA5s		**3.4**	**13.8**	**11.5**	**4.8**
	yield	0.6	2.5	1.8	4.7
HAA8s		**3.4**	**16.2**	**12.7**	**7.8**
	yield	0.6	3.0	2.0	7.6
HANs		**0.50**	**0.91**	**0.30**	**0.23**
	yield	0.1	0.2	0.1	0.22
Free chlorine UFC					
TTHMs		**291**	**237**	-	-
	yield	52	44		
HAA5s		**150**	**162**	-	-
	yield	27	30		
HAA8s		**219**	**239**	-	-
	yield	39	44		
HANs		**34.3**	**25.9**	-	-
	yield	6.1	4.7		

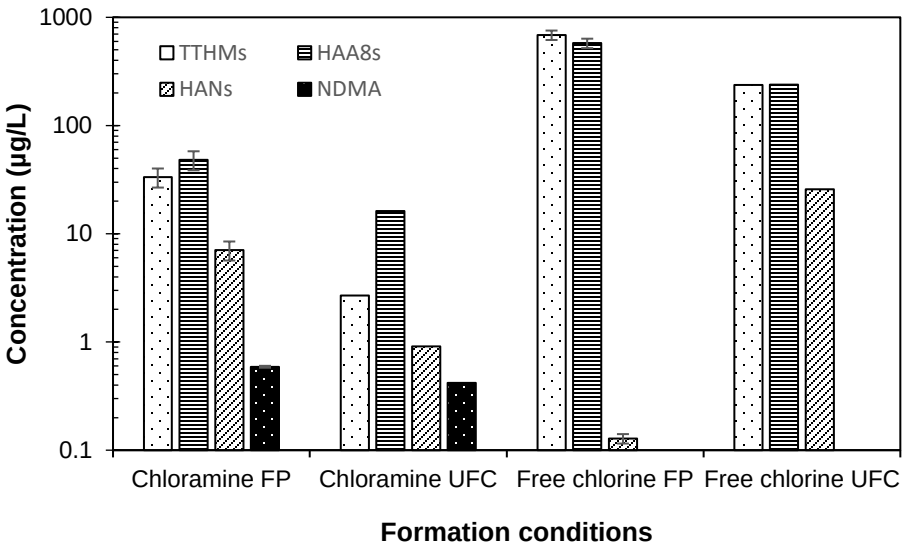

Figure 3.1: Batch WW2 DBP formation under FP and UFC conditions using chloramines and chlorine. Error bars show ± 1 RSD for FP methods.

3.1.1 NDMA formation in wastewater effluent and drinking water

High levels of NDMA were successfully formed in all three wastewaters used in this study under both FP and UFC conditions. In the absence of nitrite in the wastewater effluent, it is clear that the NDMA formation pathway is not utilizing nitrite in the process of nitrosation, but rather is more likely following the proposed unsymmetrical dimethylhydrazine oxidation pathway (Choi and Valentine, 2002; Mitch and Sedlak, 2002).

Despite consistent DOM content among WW1, WW2, and WW3, monochloramine NDMA FP showed a wider variability, ranging between 590 and 960 ng/L, representing yields between 112 and 171 ng/mg. This inconsistency between NDMA FP and TOC supports later findings in this study that NDMA precursors and bulk EfOM are not necessarily correlated. In contrast to the high NDMA FP in the wastewater effluent batches, DW1 showed only 17 ng/L FP, consistent with research that shows wastewater effluents contain higher loading of

nitrosamine precursors (Mitch and Sedlak, 2004; William A Mitch et al., 2003; Sedlak et al., 2005).

Monochloramine UFC conditions in all three wastewater batches also showed a range of formation results, between 260 and 420 ng/L with yields between 46 and 79 ng/mg. However, this was still less than half the formation seen under FP conditions on average, as is expected with the lower dose. Importantly, this level of NDMA formation under UFC conditions is still three orders of magnitude above the EPA $1x10^{-6}$ lifetime cancer risk limit, emphasizing the risk posed by precursor loading of surface waters from wastewater treatment plants and direct potable reuse without precursor control (USEPA, 2002).

NDMA formation was not tested using free chlorine since previous research has already shown NDMA yields from chlorination of wastewater effluent to be an order of magnitude less than from reaction with monochloramine (Mitch and Sedlak, 2002).

3.1.2 Effect of oxidant type on DBP formation in wastewater effluent

Monochloramine and free chlorine FP and UFC tests were performed for comparison on WW1 and WW2. Across these tests, free chlorine resulted in an order of magnitude greater TTHM and HAA8 formation than monochloramine, with consistent Cl_2 FP yields of 128 µg/mg for TTHMs and 109 µg/mg for HAA8s, compared to a range of 5.1-6.2 µg/mg for chloraminated THM FP and 9.0-10.6 µg/mg for chloraminated HAA8 FP. HAA5 yields were, on average, 78 percent of the HAA8 yields for chlorine FP, and 84 percent of the HAA8 yields for chloramine FP. The high levels of formation upon chlorination supports work done to suggest that even in low-aromatic, low-hydrophobic waters (as indicated by low SUVA and high FI values), the hydrophilic fraction still has a role in DBP formation (Hua and Reckhow, 2007; Liang and

Singer, 2003). However, it cannot be precisely distinguished from these results which fraction of DOM contributes most to the DBP formation. Overall, these results are consistent with previous studies comparing the two disinfectants, where greater formation is seen with free chlorine than monochloramine in wastewater effluent and drinking water (Bougeard et al., 2010).

This study found HAN formation to be an exception to the trend. Monochloramine FP actually formed a higher concentration of HANs than free chlorine FP (7.07 and 0.128 µg/L, respectively). The opposite was seen in UFC testing, however, where monochloramine formed only 0.5 µg/L of HANs, compared to 34.3 µg/L using free chlorine. Thus, free chlorine UFC resulted in the highest HAN formation, greater than both monochloramine UFC and free chlorine FP conditions. Bougeard et. al. (2010) and Krasner et al. (2007) have also reported low levels of HAN formation using FP tests on surface waters when using chlorine, between 0.023 and 6.2 µg/L. This behavior suggests that the extremely high chlorine dose during Cl_2 FP testing may oxidize HAN-specific precursor material before formation occurs, but that UFC doses are low enough to allow formation to proceed. As a result, free chlorine FP testing does not appear to be an effective means of measuring removal of HAN precursors.

Regardless of the oxidant used, TTHMs and HAA8s represented the highest overall DBP formation. As can be seen in Table 3.1 for WW2, slightly more HAA8s were formed than TTHMs using chloramines, while TTHMs and HAA8s were approximately equal using free chlorine.

3.1.3 Effect of oxidant dose on DBP formation in wastewater effluent

Comparing FP to UFC conditions within each oxidant type showed that UFC doses do form fewer DBPs overall than FP doses, with the exception of chlorinated HANs, as discussed

above. Monochloramine UFC formed 10-20 percent on average of the total formation potential for TTHMs, HAA8s, and HANs, while free chlorine UFC forms 35-40 percent of the FP for TTHMs and HAA8s. Thus not only does monochloramine have lower DBP formation potential overall, decreasing the chloramine dose also reduces levels of formation observed further than an equivalent decrease in Cl_2 dose. Chloraminated HAN formation was lower than chloraminated TTHM and HAA8 formation regardless of dose. This is attributable to the low DON content of the wastewater effluent as research has shown HAN FP to decrease with decreasing DON, while THM FP has been correlated more closely to SUVA (Krasner et al., 2008).

3.1.4 Effect of source water on DBP formation

Monochloramine UFC and FP tests on DW1 showed overall less absolute DBP formation than the same tests performed on the three wastewater batches due to less organic matter overall, although DBP yields per milligram of TOC were consistently higher in DW1 than the three wastewater batches. This is explained by the low TOC content of DW1. Total Br-DBP formation showed an exception to the otherwise clear difference in formation potential between drinking water and wastewater effluent. Similar levels of Total Br-DBP formation was seen in DW1 (32.8 µg/L) and WW3 (39.5 µg/L). This is likely due to the elevated bromide levels spiked in to DW1 to keep bromide constant in the blended influents later on in the study (see Table 2.1). Increased brominated DBP formation in the presence of high bromide levels is consistent with the literature (Amy et al., 1995; Bougeard et al., 2010). Despite absolute decreases in formation, the same relative trends were seen in DW1 as in wastewater effluent upon chloramination. TTHMs and HAA8s showed greater formation than HANs, and HAA8s tended to yield higher formation than TTHMs, independent of chloramine dose. Decrease in yield from chloramine FP to UFC

conditions was also comparable between wastewater effluent and drinking water. Free chlorine disinfection was not tested on DW1 since free chlorine DBP formation of drinking water is already well-understood (Krasner et al., 1989; Liang and Singer, 2003).

3.2 Batch experiments to evaluate effectiveness of different carbon types on DBP precursor removal

The effect of carbon type on NDMA precursor removal was evaluated using four different activated carbons ground to PAC size. Systematic differences were observed between NDMA FP removal and carbon pore structure characteristics. NDMA FP removals achieved by the four different carbons in PAC batch tests at the 5 mg/L dose are shown in Figure 3.2.

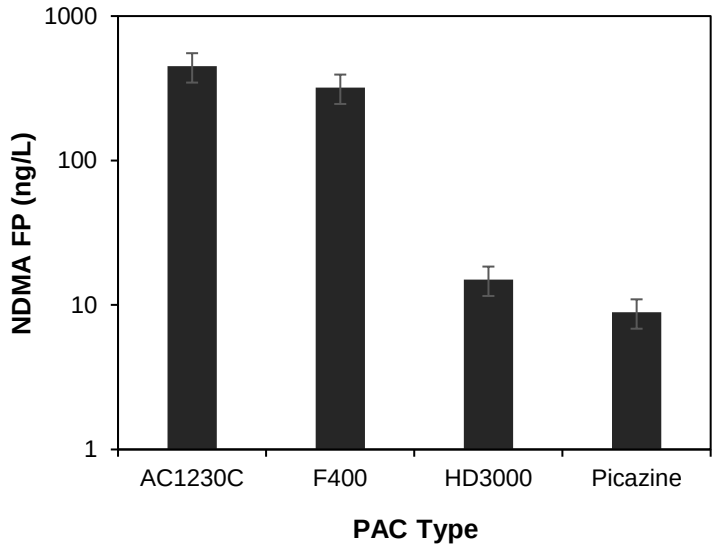

Figure 3.2: NDMA FP concentrations after treatment by various carbon types at PAC dose of 5 mg/L. Raw water NDMA FP = 960 ng/L. Error bars show ± 1 RSD for batch testing method.

3.2.1 Effect of PAC type on NDMA precursor removal

The wood-based (Picazine) and lignite-based (HD3000) carbons both achieved over 95 percent removal of the raw water NDMA FP, far outperforming the bituminous based (F400) and

coconut-based (AC1230C) carbons, which only achieved 67 and 53 percent removal, respectively. Picazine and HD3000 removals were seen to be within one RSD of each other. Additional doses of each carbon type were tested for NDMA FP removal in preliminary trials, but samples were lost during FP testing method development.

DOC removal at the 5 mg/L dose was small for all four carbons, showing less than 10 percent removal, revealing that NDMA FP is preferentially adsorbed to bulk DOM in a batch system. It is not possible to rank carbon performance according to DOC removals at the 5 mg/L dose since the standard deviation for duplicate measurements is in the same range of the level of removal achieved (Table 3.2). DOC removals at a PAC dose of 50 mg/L showed more meaningful removal results. Fractional DOC removal at a PAC dose of 50 mg/L for each carbon is also presented in Table 3.2. It is clear that the most effective carbon types for removing NDMA FP are not also the most effective for DOC removal, since F400 removes DOC better than HD3000 and Picazine at the high dose, but does not perform as well for NDMA FP at the low dose.

Table 3.2: Fraction DOC remaining for different carbon types at PAC dose of 5 and 50 mg/L, ± 1 standard deviation from duplicates. Raw water DOC = 5.9 mg/L.

Carbon type	5 mg/L	50 mg/L
AC1230C	0.971 ± 0.03	0.80
F400	0.940 ± 0.03	0.57
HD3000	0.936 ± 0.01	0.65
Picazine	0.925 ± 0.02	0.63

Differences in precursor sorption behavior among carbon types may be attributable to differences in carbon pore structures. When pore volume characteristics taken from Table 2.2 are plotted versus NDMA FP removal (using HD4000 characteristics as representative of HD3000),

a correlation can be seen between the total DFT mesopore volume (pores with widths between 20 and 360 Å) and the fractional NDMA FP removal in which the more mesoporous carbons perform better (Figure 3.3). An exponential relationship is suggested. Primary and secondary micropore volumes as well as BET surface area were also considered, but no correlation was found with NDMA FP removal.

Further analysis of the mesopore size distribution of each carbon type, based on the work of Mezzari (2006), reveals that restricting the cumulative pore volume to the pore size range of 50 to 100 Å preserves the correlation, also shown in Figure 3.3. Therefore, larger overall DFT mesopore volume could act as an indicator of larger volume within the more precise pore size range where specific NDMA precursors are being adsorbed. This evidence suggests that NDMA precursors in wastewater effluent are larger molecular weight compounds or are compounds that function in solution as having a molecular size on the order of 50 to 100 Å or greater, preventing them from accessing micropores in activated carbon. The mesopore size distribution can be seen in Figure 3.4.

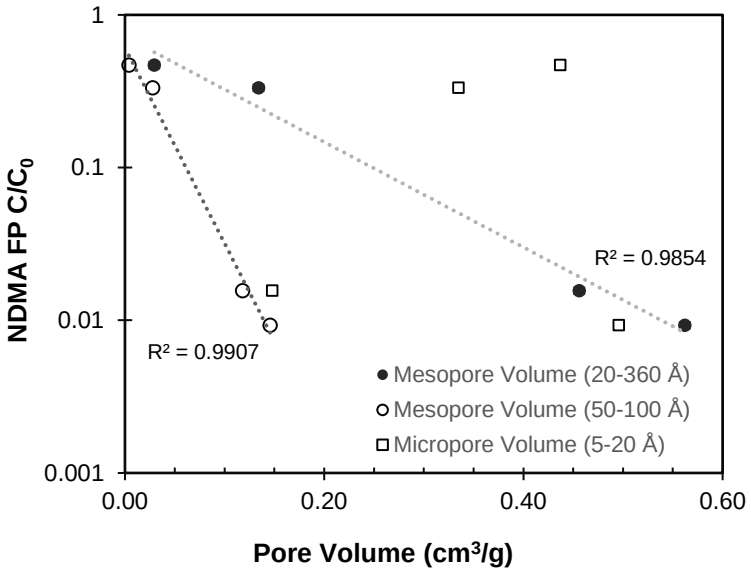

Figure 3.3: Pore volumes of four carbon types correlated to NDMA FP removal at a PAC dose of 5 mg/L.

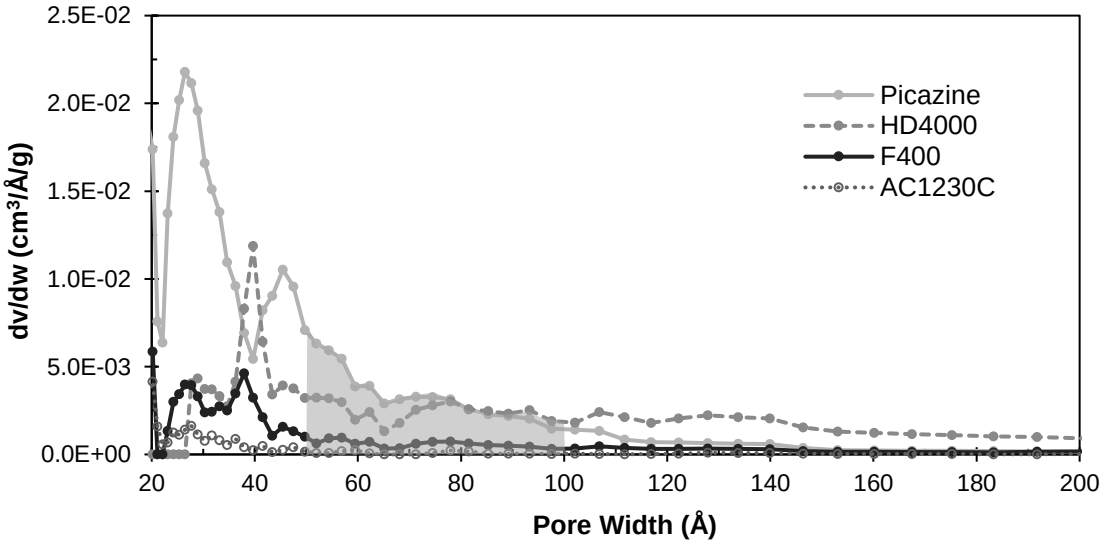

Figure 3.4: Mesopore size distribution profile for four carbon types (Mezzari, 2006)**. Shaded region to show pore size range where NDMA FP correlation holds.**

The precursors in this size range are likely extremely heterogeneous. Studies have shown a wide range of organic compounds are capable of forming NDMA upon disinfection. Soluble microbial products (SMPs) from substrate metabolism and decay of biomass in biological treatment processes are known to exist in EfOM (Barker and Stuckey, 1999) and have been shown to be potential NDMA precursors (Krasner et al., 2012, 2008; Zhang et al., 2015). These are large polysaccharide and protein-like macromolecules, with nitrogen-enriched signatures that would be adsorbed in the mesopore size range. However, high SMP content is indicated by higher levels of DON as well as characteristic fluorescence peaks in the B and T excitation-emission regions (Krasner et al., 2008). Neither of these indicators are seen in the wastewater effleunts used as influents in this study, as discussed above (Table 2.1 and Figure 2.1), suggesting that the contribution of SMPs to DBP formation in the EfOM are low. The low DON content/SMP-like peaks of the wastewater effluents, while still achieving meaningful NDMA formation and precursor removal, implies that these precursors are trace constituents of wastewater effluent, and not SMPs or compounds derived from SMPs, which would add significantly to the DON content and SMP characteristics of the water.

Given these results, it is more likely that a combination of pharmaceuticals and personal care products (PPCPs) existing at trace levels in wastewater effluent contribute the majority of NDMA FP. Numerous PPCPs detectable in wastewater effluent and containing dimethylamino moieties have been shown to form NDMA upon chloramination (Hanigan et al., 2015, 2012; Le Roux et al., 2011; Shen and Andrews, 2011, 2013). While most PPCPs yield less than 1 percent molar conversion to NDMA upon chloramine disinfection, methadone and ranitidine show exceptionally high NDMA formation yields, up to 70 and 77 percent, respectively (Hanigan et al., 2015; Shen and Andrews, 2011). Methadone alone could possibly account for up to 62

percent of NDMA FP in wastewater (Hanigan et al., 2015). The effective molecular size of these compounds in solution can be estimated using the Reddy and Doraiswany (1967) diffusivity correlation and the Stokes-Einstein equation to calculate an approximate effective radius in water. Doing so for methadone and ranitidine reveals that these compounds would have an effective diameter of 60-70 Å in solution, and thus would fall in the 50-100 Å mesopore region described above, providing further evidence toward the potential importance of these compounds in controlling NDMA precursors in wastewater effluents.

3.2.2 Effect of increasing PAC dose on DBP removal

Given that Picazine and HD3000 showed comparable removal effectiveness for NDMA FP, HD3000 was chosen for the RSSCTs in this study based on the quantity of data available from previous batch tests, but unavailable for Picazine. Dose response curves using HD3000 with WW1 are shown in Figure 3.5 through Figure 3.7.

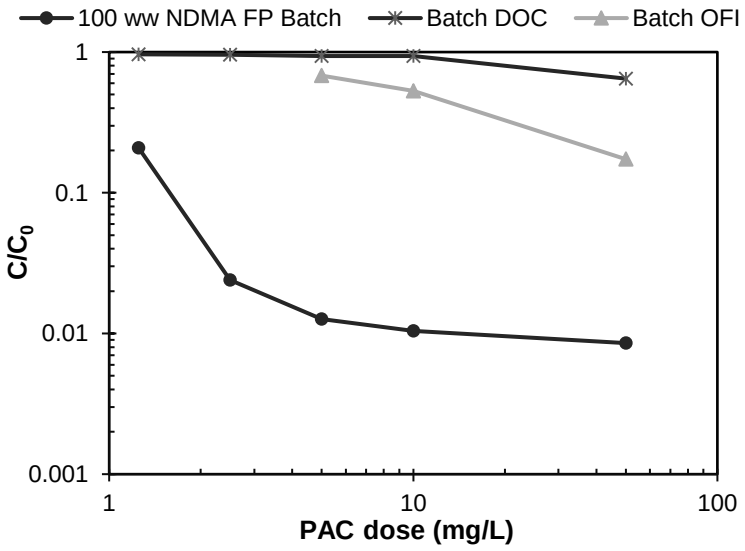

Figure 3.5: PAC batch test dose response curves for HD3000. Raw water NDMA FP = 960 ng/L, DOC = 5.9 mg/L, OFI = 1473.

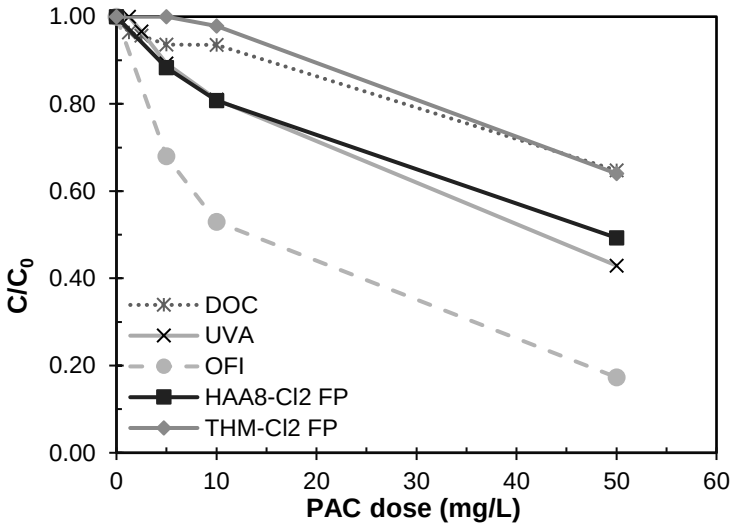

Figure 3.6: PAC removal of chlorinated DBP precursors compared to DOM. Raw water DOC = 5.8 mg/L, OFI = 1473.

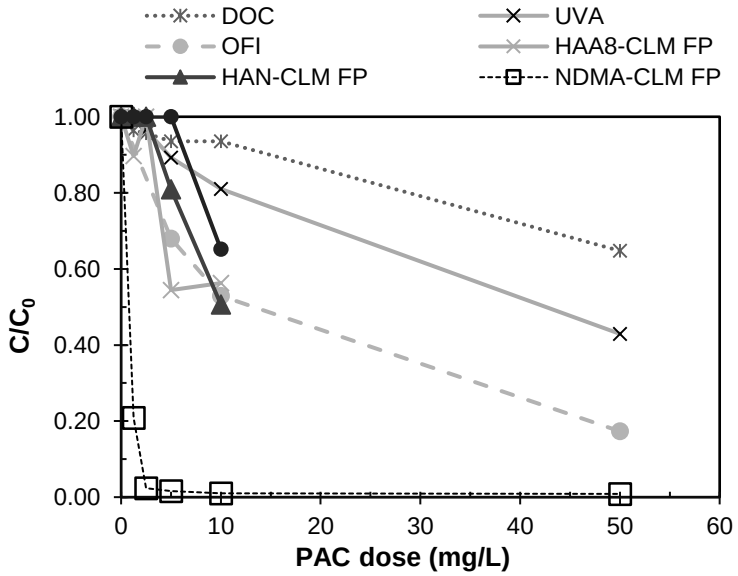

Figure 3.7: PAC removal of chloraminated DBP precursors compared to DOM. Raw water NDMA FP = 960 ng/L, DOC = 5.8 mg/L, OFI = 1473.

NDMA precursor removal. As can be seen in Figure 3.5, the majority of NDMA FP (<95 percent) is removed after a PAC dose of just 2.5 mg/L, while a small non-adsorbable fraction (about 1 percent) exists above a dose of about 10 mg/L. This is still above the reporting limit of 2.5 ng/L according to methods developed by Holady et. al. (2012). The presence of a non-adsorbable fraction above the reporting limit is evidence of a range of precursors with varying sorption behaviors. This finding is consistent with the results of Hanigan et. al. (2012) where a non-adsorbable fraction of approximately 5 percent was found above a PAC dose of 75 mg/L in wastewater effluent, leading to the conclusion that a small percentage of NDMA precursors show a low affinity for PAC.

The majority of NDMA FP in EfOM shows a very strong sensitivity to PAC dose, significantly more so than bulk DOM, as measured by DOC and fluorescence indicators (also shown in Figure 3.5). This extreme sensitivity of NDMA FP to PAC is similar to adsorbable micropollutant behavior in batch systems (Summers et al., 2013; Yoon et al., 2003) and suggests that NDMA precursors can be considered similarly, likely existing at very low concentrations in the wastewater effluent (<1 µg/L). In support of this premise, Hanigan and colleagues reported that fractional NDMA precursor removal was independent of initial precursor concentration in batch experiments (Hanigan et al., 2012; Krasner et al., 2008). Previous research on specific organic contaminant removal by PAC in batch systems has established this lack of dependence when the target compound is at trace levels providing further evidence for treating NDMA precursors like micropollutants (Graham et al., 2000; Knappe et al., 1998; Matsui et al., 2003; Westerhoff et al., 2005). Graham et. al. (2000) has also shown that when various trace organic contaminants are present, they tend not to compete with one another, but individually against

DOM for adsorption sites, which could help explain the effective removal of NDMA FP as a whole despite heterogeneous precursor material.

Interestingly, the level of removal seen in this study was better than was seen by Hanigan et al. (2012) who found that the non-adsorbable fraction was greater and a PAC dose of 15 mg/L achieved only 70 percent NDMA FP removal. By comparison, a lower dose of 10 mg/L in this study showed 99 percent removal. Hanigan and colleagues concluded that this level of removal was due exclusively to the precursor adsorbability. These findings suggest, however, that the type of PAC was likely a factor. Hanigan et. al. (2012) used a bituminous PAC in their batch testing, which this study shows to have poor NDMA FP removal capacity relative to the wood and lignite PACs, as outlined above. Thus the discrepancy in NDMA FP removal results may also be due to the smaller mesopore volume of the bituminous-based PAC used by Hanigan et. al. (2012).

TTHM, HAA8, HAN precursor removal. Removal of TTHM, HAA8, and HAN formation potential by increasing HD3000 PAC dose is presented in Figure 3.6 and Figure 3.7. Both figures show EfOM flourophores are more adsorbable by PAC than DOC measured by OFI. Removal of chlorinated and chloraminated DBP precursors generally follows these DOM indicators, as expected from past research on controlling DBP formation via removal of natural organic matter (NOM) (Clark et al., 1995; Jacangelo et al., 1995). Chlorinated THM FP closely follows DOC removal, while chlorinated HAA FP removal correlates well to UVA, as shown in Figure 3.6. OFI is removed better than chlorinated DBP FP. As discussed previously, low chlorinated HAN FP yields prevented chlorinated HAN precursor removal from being assessed.

In general, PAC doses greater than 50 mg/L would be necessary for 50 percent removal of chlorinated DBP precursors.

Chloraminated THM and HAA8 precursors were more effectively removed by PAC than chlorinated precursors in addition to showing less formation overall. At a PAC dose of 10 mg/L, only 2 percent of chlorinated THM FP was removed, in contrast to 35 percent of chloraminated THM FP. At the same dose, 19 percent of chlorinated HAA8 FP was removed and 44 percent of chloraminated HAA8 FP was removed. The mechanisms of DBP formation under chloramination are still poorly defined, so the reasons for this difference in precursor removal behavior are not well understood. However, some researchers have suggested that chloramines are more reactive with hydrophobic, humic-like compounds which are adsorbed more quickly than hydrophilic fractions (Hua and Reckhow, 2007). According to Table 3.1, WW1 has a low SUVA indicating low aromatic content and thus less hydrophobic organic matter. The hydrophobic fraction that does exist in WW1 would be more rapidly adsorbed than the hydrophilic fraction, potentially reducing the chloraminated precursors faster than chlorinated precursors. Evidence of this occurring can be seen in the changing ratio of B and T to A and C fluorescence peaks with increasing PAC dose. A and C peaks are more humic-like while B and T peaks are more protein like, thus as the (B+T)/(A+C) ratio increases, more A and C peaks are being removed relative to B and T peaks. This behavior can be seen for HD3000 in Figure 3.8.

As a result, removal of OFI was found to be a good indicator of decreasing FP for chloraminated DBPs (Figure 3.7), owing to the fact that OFI is dominated by humic-like A and C peaks and thus a good measure of the hydrophobic fraction of wastewater. This suggests that chloraminated DBP precursors are within the subset of EfOM that is described by fluorescence spectroscopy. Chloraminated HAA8 and HAN precursors showed insignificant differences in

removal behavior, while chloraminated THM FP was slightly more resistant to removal at low doses. Overall, doses of 10 to 20 mg/L are necessary for 50 percent removal of chloraminated THM, HAA8, and HAN precursors.

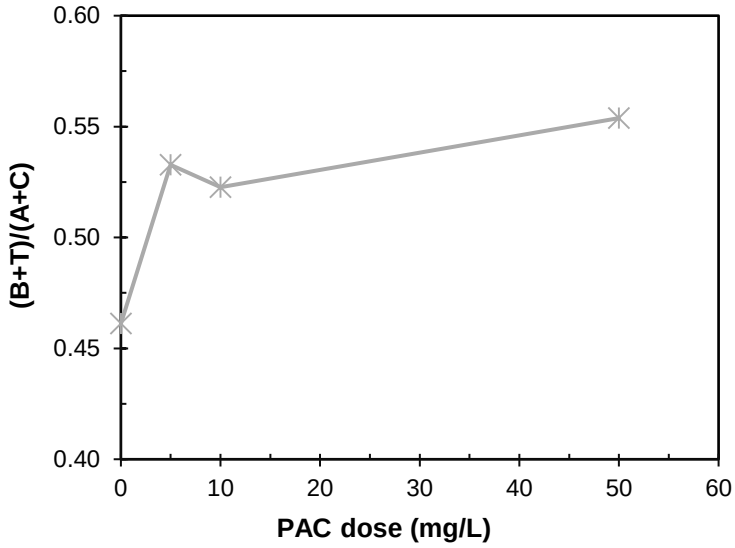

Figure 3.8: Ratio of B and T peaks to A and C peaks with increasing PAC dose.

3.3 Preliminary RSSCTs to evaluate effect of Empty Bed Contact Time on DBP precursor removal

RSSCTs were run using 10- and 20-minute simulated full-scale EBCTs to evaluate the effect of GAC contact time on adsorption capacity. The 20-minute column exhibited better removal behavior at longer contact times for most EfOM DBP precursors as well as for bulk organic matter. Breakthrough curves are shown in Figure 3.9 through Figure 3.11 for NDMA and chlorinated/chloraminated TTHMs, HAA8s, and HANs. Table 3.3 and Table 3.4 summarize these results.

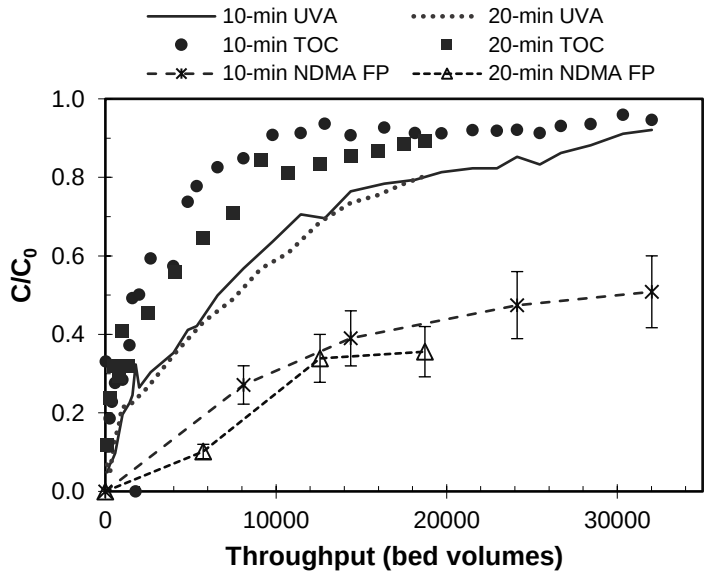

Figure 3.9: Normalized breakthrough of TOC, UVA, and NDMA FP for 10 and 20 minute EBCTs. Raw water TOC = 5.28 mg/L, UVA = 0.102 cm^{-1}, NDMA FP = 590 ng/L. Error bars show ± 1 RSD for NDMA FP method after RSSCT.

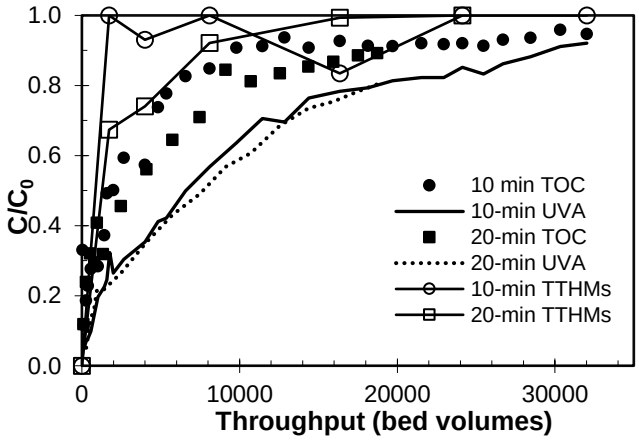

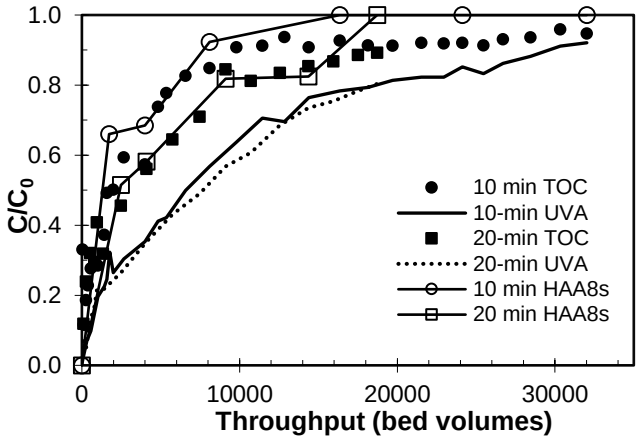

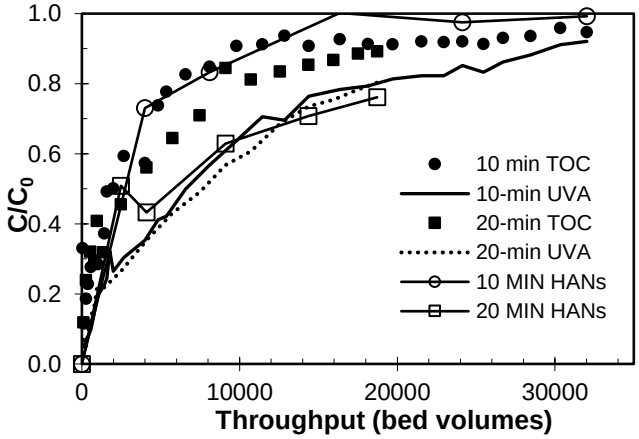

Figure 3.10: TTHM, HAA8, and HAN monochloramine formation potential breakthrough curves compared to TOC and UVA for 10 and 20 minute EBCTs. Raw water TOC = 5.28 mg/L, UVA = 0.102 cm-1, TTHM FP = 33.4 µg/L, HAN FP = 7.07 µg/L, HAA8 FP = 48.2 µg/L

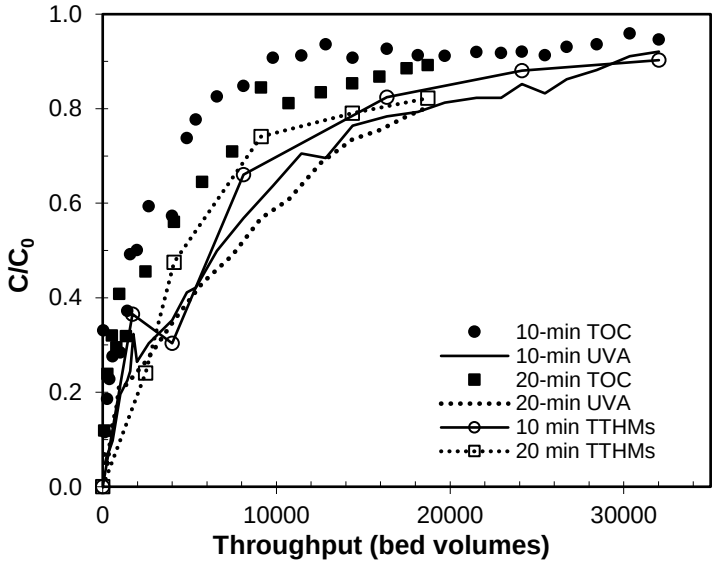

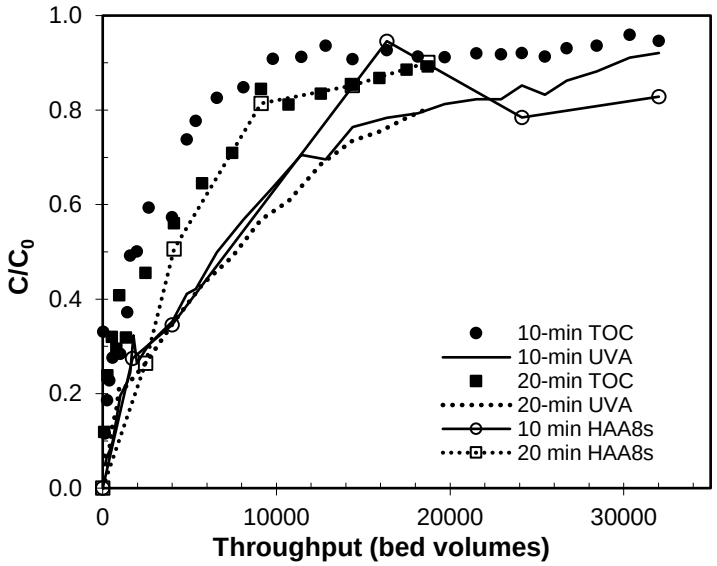

Figure 3.11: TTHM, HAA8, and HAN free chlorine formation potential breakthrough curves compared to TOC and UVA for 10 and 20 minute EBCTs. Raw water TOC = 5.28 mg/L, UVA = 0.102 cm-1, TTHM FP = 686 µg/L, HAA8 FP = 577 µg/L

Table 3.3: Approximate throughput in bed volumes to 20 and 50 percent breakthrough for TOC, UVA, and NDMA FP in both 10 and 20 minute EBCT columns.

	10-minute EBCT	20-minute EBCT
TOC BV_{20}	300	210
UVA BV_{20}	1100	900
NDMA FP BV_{20}	6000	8500
TOC BV_{50}	1980	3000
UVA BV_{50}	6600	7600
NDMA FP BV_{50}	29500	>30000

Table 3.4: Throughputs in bed volumes to 20 and 50 percent breakthrough for chloraminated and chlorinated DBP FP in both 10 and 20 minute EBCT columns.

	10-minute EBCT	20-minute EBCT
Monochloramine FP:		
TTHM BV_{20}	<500	<500
HAA8 BV_{20}	500	900
HAN BV_{20}	<900	900
TTHM BV_{50}	<1000	1000
HAA8 BV_{50}	1200	2300
HAN BV_{50}	<2400	2400
Free chlorine FP:		
TTHM BV_{20}	900	2100
HAA8 BV_{20}	1200	1900
TTHM BV_{50}	6200	4600
HAA8 BV_{50}	7000	4000

3.3.1 Effect of EBCT on EfOM removal

The 20-minute column generally performed better than the 10-minute column for both DOM and NDMA FP. The exception to this trend occurs for TOC and UVA early on in the run, where the 10-minute column was the same as or slightly more effective than the 20-minute

column. The 20-minute column did not begin to show better TOC removal than the 10-minute column until approximately 40 percent breakthrough, or 1000 BV. The difference between the two EBCTs is more clearly seen at 50 percent breakthrough. In the 10-minute column, 50 percent TOC breakthrough occurred at approximately 1980 BV, while in the 20-minute column, 50 percent TOC breakthrough occurred at approximately 3000 BV. Thus, the 20-minute EBCT column was approximately 52 percent more effective than the 10-minute EBCT column in TOC removal to BV_{50}. This difference was not as pronounced for UVA breakthrough. The 20-minute column only showed a 15 percent improvement on UVA removal from the 10-minute column.

This data is consistent with previous work showing longer EBCTs to result in better removal of DOM in drinking water (Bond and Digiano, 2004; Zachman and Summers, 2010; Zachman et al., 2007). EfOM does tend to break through the zone of mass transfer more rapidly than drinking water applications and models. Bond and Digiano (2004) reported an average BV_{50} value of 5,068 for TOC from 116 full-scale trials using 8x30 GAC size (see HD3000 full scale properties, Table 2.2) compared to an average BV_{50} of 2490 for both EBCTs used in this study. Research has shown that PD-RSSCTs accurately predict background organic matter removal at full scale, thus comparing these BV_{50} values is warranted (Crittenden et al., 1991).

3.3.2 Effect of EBCT on NDMA precursor removal

Effective removal of NDMA FP was seen in both the 10-minute and 20-minute EBCT columns. NDMA FP removal was consistently better in the 20-minute column, even at early throughputs, reaching 20 percent breakthrough at 8500 BV, while the 10-minute column reached BV_{20} at approximately 6000 BV. Thus, the 20-minute EBCT column was approximately 42 percent more effective than the 10-minute EBCT column to 20 percent breakthrough. 50 percent

breakthrough in the 20-minute column was not reached during the run time, but the 10-minute column approached BV_{50} at approximately 29500 BV. Thus, although at certain points in the breakthrough curve the 10- and 20-minute column values are within one RSD of each other, this data strongly suggest that NDMA precursors are more effectively removed by longer EBCTs to at least 50 percent breakthrough; EBCT dependence beyond 50 percent breakthrough is unknown. Corwin and Summers have shown that trace organic contaminants can exhibit an EBCT dependence relative to percent breakthrough, where longer EBCTs are only more effective at early breakthrough times (Corwin and Summers, 2012; Summers et al., 2013). Zietzschmann et al. (2014) partially observed this in wastewater effluents using RSSCTs, although the percent breakthrough where changing EBCT dependency occurred was delayed to almost 60 percent, and run times were not sufficient to fully observe the effect. Thus if NDMA precursors are to be considered as micropollutants, it is unclear whether the EBCT relationship seen over the duration of this study would hold true during longer breakthrough times. Very little other work has been done using RSSCTs as a tool for evaluating specific organic contaminant removal in wastewater effluent and as such the effect of EBCT in waters with strongly competing EfOM is not well-understood. Overall, it is possible that when treating wastewater effluent, increased competition increases the time that the mass-transfer zones of target adsorbates and bulk organic matter overlap, allowing longer EBCTs to be effective at longer throughputs. Thus the changing dependency of EBCT for trace organic constituents may not be observed during the useful runtime of GAC columns treating EfOM.

Both EBCTs removed NDMA precursors significantly better than TOC and UVA, consistent with findings from batch testing. For example, NDMA FP reached 20 percent breakthrough in both EBCTs 5 to 10 times later than UVA. Overall, when considering the

average ratio from all NDMA FP data points at greater than 10 percent breakthrough, the 10 and 20-minute EBCTs both removed NDMA FP about 14 times more effectively than TOC at the bench scale according to column throughputs. Normalized concentration breakthroughs of TOC, UVA, and NDMA FP with throughput in bed volumes are plotted in Figure 3.9. Table 3.3 summarizes throughput to 20 percent and 50 percent breakthrough for TOC, UVA, and NDMA FP in both columns.

3.3.3 *Effect of EBCT on TTHM, HAA8, and HAN precursor removal*

Chloraminated DBPs. Breakthrough data for chloraminated DBP precursors is presented in Figure 3.10. Throughputs to 20 and 50 percent breakthrough for each precursor type are summarized in Table 3.4. As can be seen in Figure 3.10, the 20-minute column showed better performance for removal of chloraminated DBP precursors than the 10-minute column. Chloraminated THMs showed 100 percent breakthrough in less than 2000 BV in the 10-minute column, while the 20-minute column did not break through entirely until approximately 16000 BV. Breakthrough was still considerably faster than TOC, however, showing 50 percent in the effluent in approximately 1000 BV. Thus, chloraminated THM precursors in EfOM are relatively poorly adsorbed in the flow-through columns. TOC did represent a good indicator for chloraminated HAA8 FP removal, however, with almost a one-to-one breakthrough relationship. Similarly, chloraminated HAN FP closely followed TOC in the 10-minute column. In the 20-minute column, TOC was a conservative indicator of HAN FP breakthrough, while normalized effluent UVA actually showed a better fit.

Chlorinated DBPs. Chlorinated THM FP was much better adsorbed than chloraminated THMs, reaching 50 percent breakthrough at approximately 6200 and 4600 BV for the 10- and

20-minute columns, respectively, and did not reach complete breakthrough during the three-week run-time (Figure 3.11, top). Normalized effluent UVA proved to be a good surrogate for THM precursor breakthrough (making TOC breakthrough a conservative indicator), consistent with previous applications in surface waters (Bougeard et al., 2010; Goslan et al., 2002). This helps establish that EfOM precursors behave very similarly in GAC as in drinking water applications.

Chlorinated HAA8 FP showed similar breakthrough shape as THM FP, also achieving better removal than chloraminated HAA8 FP in both EBCTs (Figure 3.11, bottom). Chlorinated HAA8 FP reached 50 percent breakthrough at approximately 7000 and 4000 BV in the 10 and 20-minute columns, respectively. UVA breakthrough predicted chlorinated HAA8 FP best in the 10-minute column, while TOC predicted chlorinated HAA8 FP best in the 20-minute column. Regardless, this data shows a clear relationship between removal of bulk organic matter and removal of carbonaceous DBP precursors in wastewater EfOM. As has been previously discussed, chlorinated HAN FP showed insignificant and inconsistent FP values, potentially due to oxidation of the precursors before DBP formation during the chlorination hold-time, and thus breakthrough data was unavailable.

Comparison. BV_{20} and BV_{50} results from chlorine and chloramine FP tests on 10- and 20-minute EBCT column effluents are summarized in Table 3.4. Generally, chlorinated and chloraminated TTHM, HAA8, and HAN FPs all follow the same trend as bulk DOM breakthrough on a normalized concentration basis, as measured by TOC and UVA. Chlorinated DBP precursors are slightly better removed in the flow-through system than chloraminated DBPs. These results are in contrast to what was seen during batch testing, which showed that chloraminated DBP precursors are generally better adsorbed than TOC and UVA and chlorinated

precursors. It was hypothesized that chloraminated precursors may be more hydrophobic and therefore more strongly adsorbing in the batch system. Chlorinated DBP precursors, on the other hand, do not show any difference between batch and column tests. This behavior is not well understood, but suggests that fouling in the flow-through column may have an effect on chloraminated DBP precursors but not on chlorinated precursors. Fouling can occur in the flow-through GAC column system but not in a PAC batch system as a result of myriad factors, including increased particle size (Corwin and Summers, 2010; Summers et al., 1989). If so, monochloramine is potentially reacting with precursors in the organic matter present that are distinct from chlorinated precursors and that compete with TOC. Thus, while it appears that chloraminated DBP FP is directly linked to TOC and UVA in Figure 3.10, this may be a coincidental result of a shift in the adsorption capacity of PAC to GAC. In contrast, the consistent behavior of chlorinated DBP precursors across the batch and column experiments points toward it being directly associated with the bulk organic matter, and therefore unsusceptible to fouling effects. Finally, the 20-minute column generally performed better for chloraminated DBPs while the 10-minute column performed slightly better for chlorinated DBPs.

These results also further illuminate the removal behavior of NDMA precursors by GAC in the presence of EfOM. None of the chlorinated or chloraminated DBP precursors showed similar behavior to NDMA FP. This is additional evidence for considering NDMA precursors as distinct trace compounds in wastewater effluent, and not as a nitrogenous subset of overall DOM. This is consistent with work done by Chen and Westerhoff in which models using DOC and UVA inputs were able to accurately predict TTHM, HAA9, and HAN formation potential in a variety of water types, but unable to predict NDMA formation (Chen and Westerhoff, 2010).

DON has also been shown to have a poor correlation to NDMA FP, furthering this interpretation (Krasner et al., 2008)

3.4 RSSCTs to evaluate the effect of blending on DBP precursor removal

Using wastewater effluent blended with a coagulated non-wastewater impacted drinking water source (WW3 and DW1, Table 3.1) in additional RSSCTs provided information about the adsorption behavior of wastewater-derived precursors in the presence of NOM and at levels of wastewater influence likely to be seen in drinking water contexts. NDMA FP breakthrough data for blended waters is presented in Figure 3.12 and Figure 3.13. Chloraminated TTHM, HAA8, and HAN FP breakthrough data is presented in Figure 3.14. These results are summarized in Table 3.5 and discussed below.

Table 3.5: Approximate throughputs in bed volumes to 20 and 50 percent breakthrough for DOM and chloraminated DBP FP in blended influents.

	100ww	**60ww/40dw**	**20ww/80dw**	**100dw**
TOC BV_{20}	300	700	1400	3500
TTHM FP BV_{20}	600	600	1900	4300
HAA8 FP BV_{20}	900	1600	2000	5000
HAN FP BV_{20}	800	1100	2700	8300
UVA BV_{20}	700	1300	3300	5800
OFI BV_{20}	5000	6800	9000	4000
NDMA FP BV_{20}	11600	9300	12600	-
TOC BV_{50}	2200	3400	6200	12700
TTHM FP BV_{50}	2500	2500	5500	15000
HAA8 FP BV_{50}	3800	7800	6200	19700
HAN FP BV_{50}	4700	5700	8400	17200
UVA BV_{50}	4800	9100	14600	19700
OFI BV_{50}	17000	22500	32300	36000
NDMA FP BV_{50}	32000	31000	39600	-

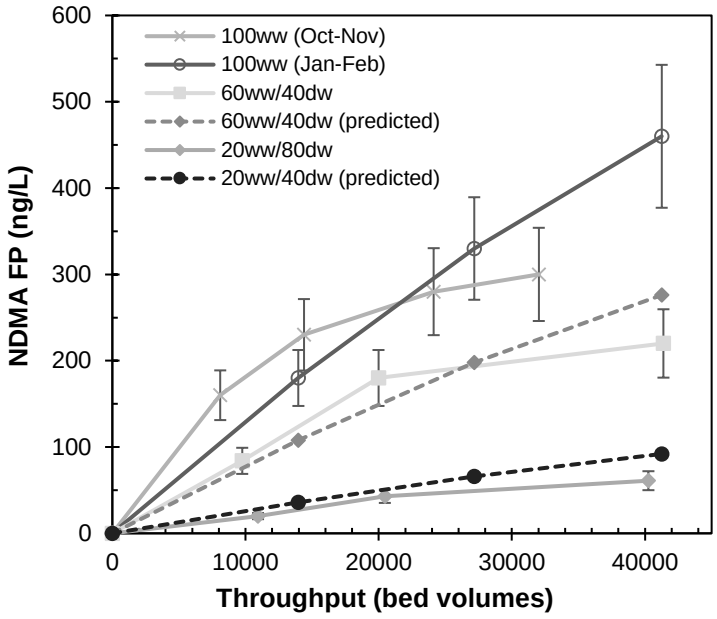

Figure 3.12: NDMA FP breakthrough of three blended waters. 100ww (Oct-Nov) NDMA FP = 590 ng/L, TOC = 5.28 mg/L; 100ww (Jan-Feb) NDMA FP = 747 ng/L, TOC = 6.1 mg/L; 60ww/40dw NDMA FP = 400 ng/L, TOC = 4.1 mg/L; 20ww/80dw NDMA FP = 120 ng/L, TOC = 2.2 mg/L. Error bars show ± 1 RSD for NDMA FP after RSSCT.

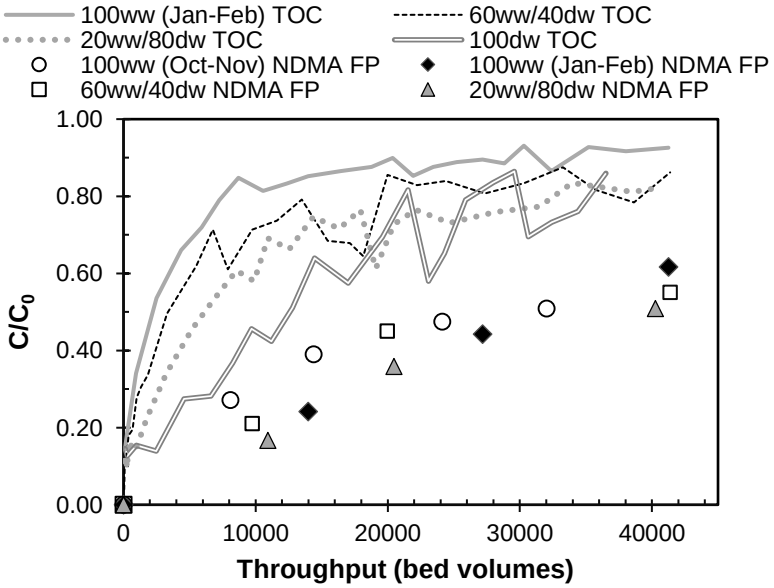

Figure 3.13: Normalized TOC and NDMA FP breakthrough for range of blended waters. 100ww (Oct-Nov) NDMA FP = 590 ng/L, TOC = 5.28 mg/L; 100ww (Jan-Feb) NDMA FP = 747 ng/L, TOC = 6.1 mg/L; 60ww/40dw NDMA FP = 400 ng/L, TOC = 4.1 mg/L; 20ww/80dw NDMA FP = 120 ng/L, TOC = 2.2 mg/L; 100dw NDMA FP = 37 ng/L, TOC = 1.0 mg/L.

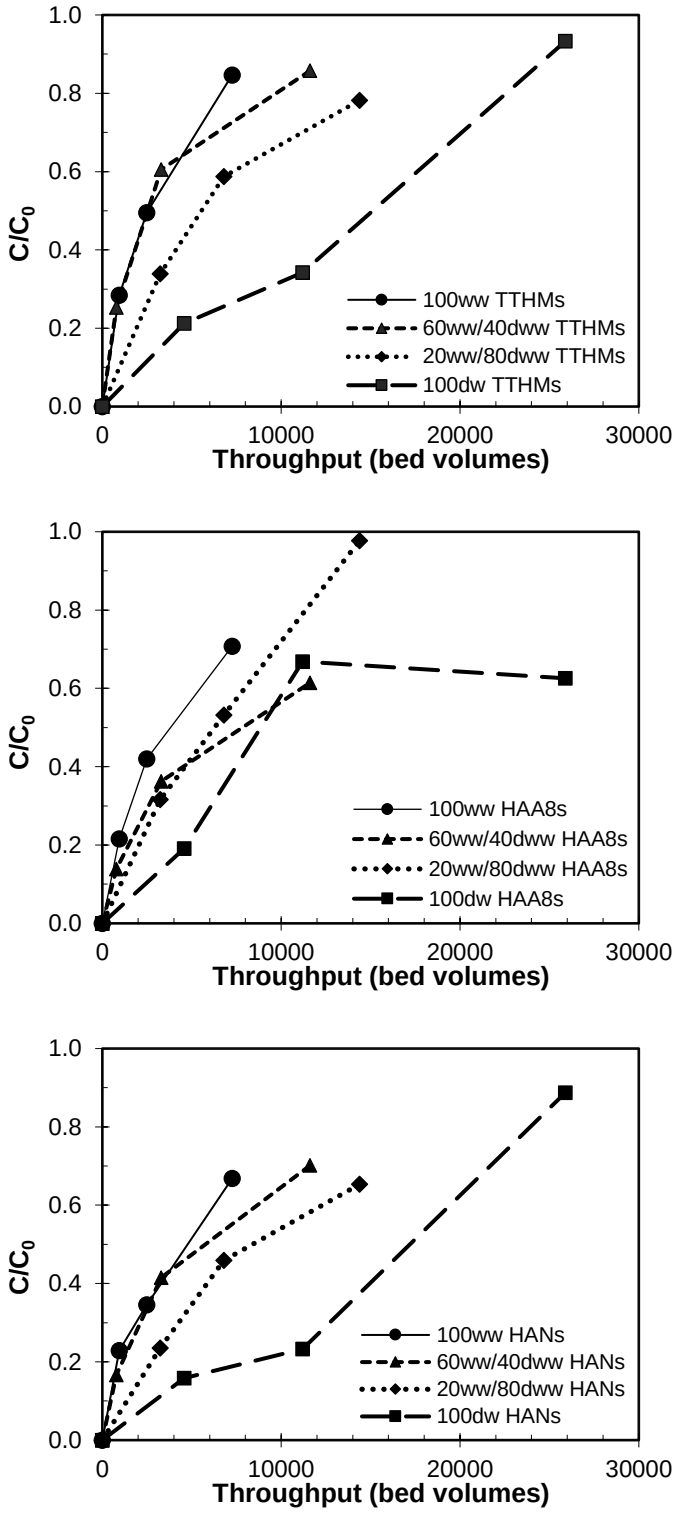

Figure 3.14: Breakthrough of chloraminated TTHMs, HAA8s, and HANs for varying wastewater content influents.

3.4.1 Effect of blending on NDMA precursor removal

Using wastewater effluent blended with a coagulated non-wastewater impacted drinking water source in additional RSSCTs (WW3 and DW1, Table 3.1) revealed linear mass-balance removal behavior among the NDMA precursors. Figure 3.12 shows the results for the three RSSCTs run with the three different wastewater effluent ratios: 100ww, 60ww/40dw, and 20ww/80dw. NDMA FP results from the preliminary RSSCT to identify the effect of EBCT (10-minute EBCT, 100ww) are also included in Figure 3.12 for comparison. Even though this column was run using a different shipment of CCWRD wastewater effluent (WW2), it is consistent with the removal behavior in the WW3 experiments and breakthrough results are clearly within one RSD of each other.

Predicted values were calculated using a mass balance approach based on the effluent concentrations of the 100ww column. It is clear from Figure 3.12 that the experimental breakthrough curves for the 60ww/40dw and 20ww/80dw columns follow the predicted values; most of the experimental breakthrough values for the blended waters are within one RSD of the predicted values, which does not include the inherent error in the predictions. Thus NDMA precursors can be considered as conservative tracer compounds of wastewater EfOM and do not change their sorption behavior in diluted solutions or in the presence of NOM. That is, NOM does not cause any significant or additional pore blockage of GAC particles beyond the effects of EfOM. It is also clear that increasing the wastewater effluent to drinking water ratio increases the rate of breakthrough. This is relevant on a mass concentration basis, as presented in Figure 3.12, for utilities potentially concerned about meeting NDMA levels below a specific MCL. Although the FP concentrations displayed in Figure 3.12 are unrealistically high for utility scenarios, one UFC test performed on the 100ww column effluent after 41,250 bed volumes yielded 36 ng/L of

NDMA (compared to 420 ng/L formed at the same throughput using an FP dose), which is still two orders of magnitude higher than the EPA suggested $1x10^{-6}$ lifetime cancer risk limit for NDMA in drinking water (USEPA, 2002). Thus, NDMA precursors break through at levels relevant to public health in advance of 40,000 bed volumes in 100 percent wastewater systems.

TOC also breaks through sooner as the proportion of wastewater effluent increases. This behavior is to be expected both due to the increased precursor load and greater background organic matter increasing the rate of exhaustion of the mass transfer zone and competition for adsorption sites in higher wastewater content waters. Figure 3.13 shows this behavior for TOC and NDMA FP on a normalized basis. NDMA FP testing was not performed on the 100 percent drinking water column since the influent FP was low (17 ng/L) and appreciable breakthrough would likely not have been seen during the study duration. As can be seen, the fractional concentration of TOC in the column effluent increases more rapidly with increasing wastewater effluent ratio in the influent, as shown by the slopes of the breakthrough curves, especially before 15000 BV.

This relationship is much less pronounced for NDMA FP breakthrough. On a normalized basis, the concentrations of the four RSSCT data sets in Figure 3.13 (two blends and two trials of 100ww) show similar breakthrough behaviors and the curves overlap significantly. Until approximately 40 percent breakthrough, three out of four of the columns follow the expected trend of earlier breakthrough with increasing influent TOC. The October-November 100ww (WW2), 60ww/40dw, and 20ww/80dw columns reach 20 percent NDMA FP breakthrough at approximately 6000 BV, 9500 BV, and 12800 BV, respectively. This is a 113 percent increase in NDMA FP removal effectiveness from the 100ww column to the 20ww/80dw column, compared to a 409 percent increase in removal effectiveness for TOC between the same columns at the

same 20 percent breakthrough point. Thus, dilution of the wastewater effluent has less of an effect on NDMA precursors than on TOC in the normalized breakthrough. This relative sensitivity of TOC and NDMA FP to initial TOC concentration is expressed in Figure 3.15. As can be seen by the slope of the TOC relationship to the slope of the NDMA FP relationship, increasing TOC_0 values (a measure of wastewater content) affect NDMA FP breakthrough less dramatically than TOC breakthrough. This inverse dependence on influent TOC has also been shown by Summers et al. (2013). The uniqueness of the NDMA FP best-fit line compared to that TOC in Figure 3.15 has further implications for considering NDMA precursors like micropollutants, as will be discussed in the next section.

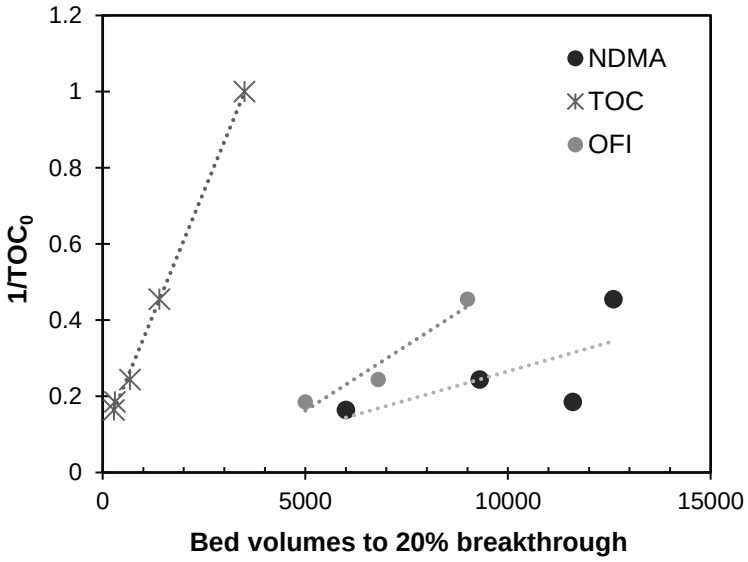

Figure 3.15: Throughput in bed volumes to reach 20 percent breakthrough for TOC, NDMA FP, and OFI correlated to influent TOC.

The January-February 100ww (WW3) trial does not follow the pattern of the first three columns explained above, and shows better removal than is expected even though the TOC and UVA breakthrough data comparing the two 100ww trials is consistent. One possible explanation

for this difference in behavior is biodegradation of precursors occurring in the January-February 100ww trial. The three- to four-week runtime could allow the growth of biofilm in the column and contribute an additional removal mechanism to adsorption. However, further analysis and experimentation suggest this is unlikely. Although some biodegradation of TOC was seen in the RSSCTs for certain trials, noticeable in the decrease in the 60ww/40dw TOC line below the overall breakthrough trend between approximately 12000 and 18000 BV in Figure 3.13, this degradation was found to occur primarily in the glass-wool prefilter which was replaced with a clean prefilter if this characteristic drop in TOC was seen to occur. When a clean prefilter was installed, the TOC breakthrough returned to normal levels. Biodegradation of TOC was not seen in the January-February 100ww trial. Furthermore, even if it were occurring, it was found that removal potential of NDMA FP by biodegradation alone is insignificant compared to adsorption. This was determined in additional bench scale biofiltration experiments outlined in Appendix A3.

Thus, although the exact reasons behind this differing sorption behavior in the January-February 100ww trial using WW3 are not well understood, Figure 3.15 clearly expresses the general relationship between influent TOC concentration (representative of the higher background EfOM) and throughput to 20 percent breakthrough for NDMA FP and TOC in the blended trials: increasing the influent TOC concentration decreases the time to breakthrough.

Evidence for micropollutant behavior. The overall lack of a strong effect of initial NDMA FP on the normalized concentration breakthroughs could be another indicator of micropollutant behavior of NDMA precursors. As previously discussed, research has shown that trace organic contaminants at extremely low influent concentrations show a lack of sensitivity to influent concentration when measuring normalized removal by PAC in batch systems (Graham et

al., 2000; Knappe et al., 1998; Matsui et al., 2003; Westerhoff et al., 2005). This independence is explained by a linear equilibrium isotherm at extremely low influent concentrations, generally less than a microgram per liter, developed theoretically by Kilduff et. al. (1998) and has also been observed in continuous-flow adsorption columns (Corwin and Summers, 2012; Summers et al., 2013).

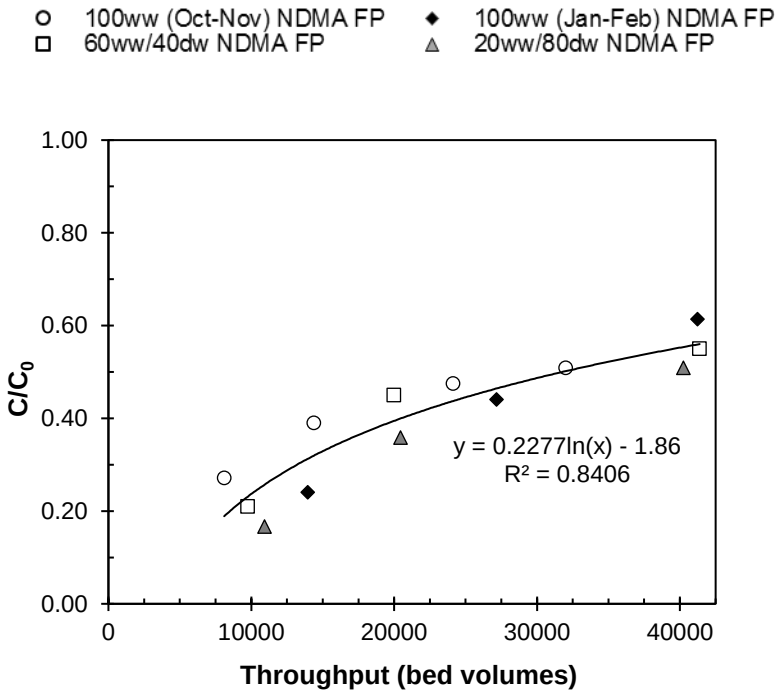

Figure 3.16: Normalized NDMA FP breakthrough data considered together. Proposed model valid for TOC_0 = 2.2-6.1 mg/L and NDMA FP_0 = 120-747 ng/L.

As previously mentioned, Hanigan et. al. (2012) has already shown NDMA precursor removal to be independent of initial precursor concentration in batch experiments. Thus it is likely that the linear isotherm effect is also occurring in this case, but not clearly distinguishable from the simultaneously changing TOC concentration occurring during dilution. The effect of the wide range of influent conditions (i.e., varying TOC:NDMA precursor ratios) on NDMA FP

removal is clearly diminished in the normalized breakthrough in Figure 3.13, however, which lends itself to the micropollutant hypothesis. Given this lack of a strong dependence on influent conditions, a potential relationship between normalized breakthrough and throughput can be developed if all the NDMA FP values are considered together as one data set. A general trend can be seen to exist within a specific envelope in Figure 3.16. This does not suggest that initial TOC has no effect, but that its effect is slight enough that a general trend appears among all the blended waters.

The correlation presented in Figure 3.16 could be used to predict NDMA precursor removal within a specific set of influent conditions by lignite-based GAC at the bench scale. Using nonlinear regression analysis, a logarithmic correlation has been developed. This relationship has a high coefficient of determination of 0.84 within the boundary conditions of influent ranges tested in this study. Thus for wastewater impacted source waters with TOC_0 in the range of 2.2-6.1 mg/L and NDMA FP_0 in the range 120-747 ng/L the following equation provides an estimate of NDMA precursor breakthrough:

$$\frac{[\boldsymbol{NDMA\ FP}]}{[\boldsymbol{NDMA\ FP_0}]} = \mathbf{0.2277}\ \mathbf{ln}(\boldsymbol{BV}) - \mathbf{1.86} \qquad (2)$$

Potential of fluorescence indicators for predicting NDMA FP. Another method for predicting NDMA FP breakthrough may be the use of fluorescence spectroscopy to measure the wastewater "fingerprint" of GAC effluent. Fluorescence EEMs were developed for select breakthrough points of each RSSCT. Multiple parameters from fluorescence EEMs were correlated to NDMA FP breakthrough, including A, C, B, and T peak intensities and OFI.

Although Peaks B and T were predicted to potentially be better indicators of NDMA precursors for their higher nitrogen content, it was found that OFI showed as good of a fit or better when fluorescence intensity breakthroughs were plotted simultaneously with NDMA FP breakthrough. The similarity of the breakthrough relationships can be seen in Figure 3.17. This similarity is maintained when data is normalized to influent concentration/intensity. Thus it is apparent that OFI also follows a linear mass balance behavior in the flow-through GAC columns after blending and could be considered as a proxy indicator of NDMA precursor content in EfOM. OFI breakthrough also exhibits a similar dependence on initial TOC concentration, as can be seen in Figure 3.15. Increasing breakthrough is inversely correlated to influent TOC according to approximately the same slope as NDMA FP.

Further evidence for the use of OFI as a surrogate exists in the strong relationship between the GAC surface loading rates (q) of OFI and NDMA FP, while no such relationship exists for NDMA FP and TOC, as can be seen in Figure 3.18. Nonlinear regression analysis reveals that $q_{\text{NDMA FP}}$ and q_{OFI} are related by a power function such that:

$$\boldsymbol{q_{NDMA\,FP} = 4 \times 10^{-4} (q_{OFI})^{1.7257}} \quad (3)$$

Data points used to develop Equation 3 in Figure 3.18 were taken from all OFI samples from both batch and column tests, blended and non-blended, where the carbon use rate (CUR) or PAC dose matched that of NDMA FP samples. Thus this behavior is consistent across the batch and flow-through systems. Even though OFI removal does not mirror NDMA FP removal on a normalized concentration basis in the batch system (Figure 3.5), the surface loading relationship suggests that the fluorescence intensity of NDMA precursors is low relative to the fluorescence intensity of the bulk organic matter remaining in the water, such that the relationship is hidden

when only considering the water phase concentrations. When considering the surface phase concentration, however, it becomes apparent that the GAC increasingly adsorbs NDMA precursors as it adsorbs overall fluorescence, even in the batch system. The non-linear relationship and lack of a strong relationship with B and T peaks relative to A and C peaks, however, is evidence against the conclusion that OFI measures NDMA precursors themselves. Rather, it is likely that fluorescent organic matter is simply more strongly adsorbing than TOC, and thus has comparable adsorbability to NDMA precursors.

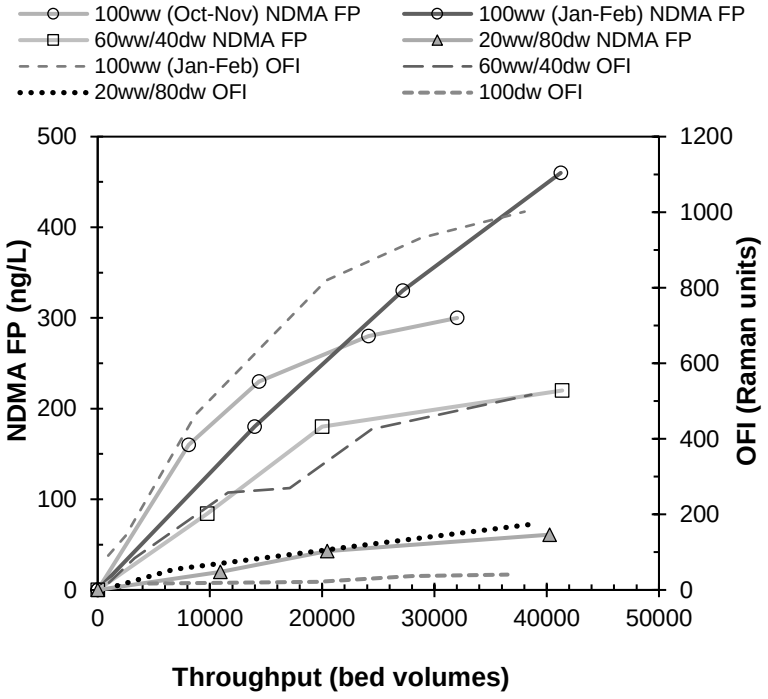

Figure 3.17: Comparison of OFI intensity breakthrough to NDMA FP breakthrough for all RSSCTs.

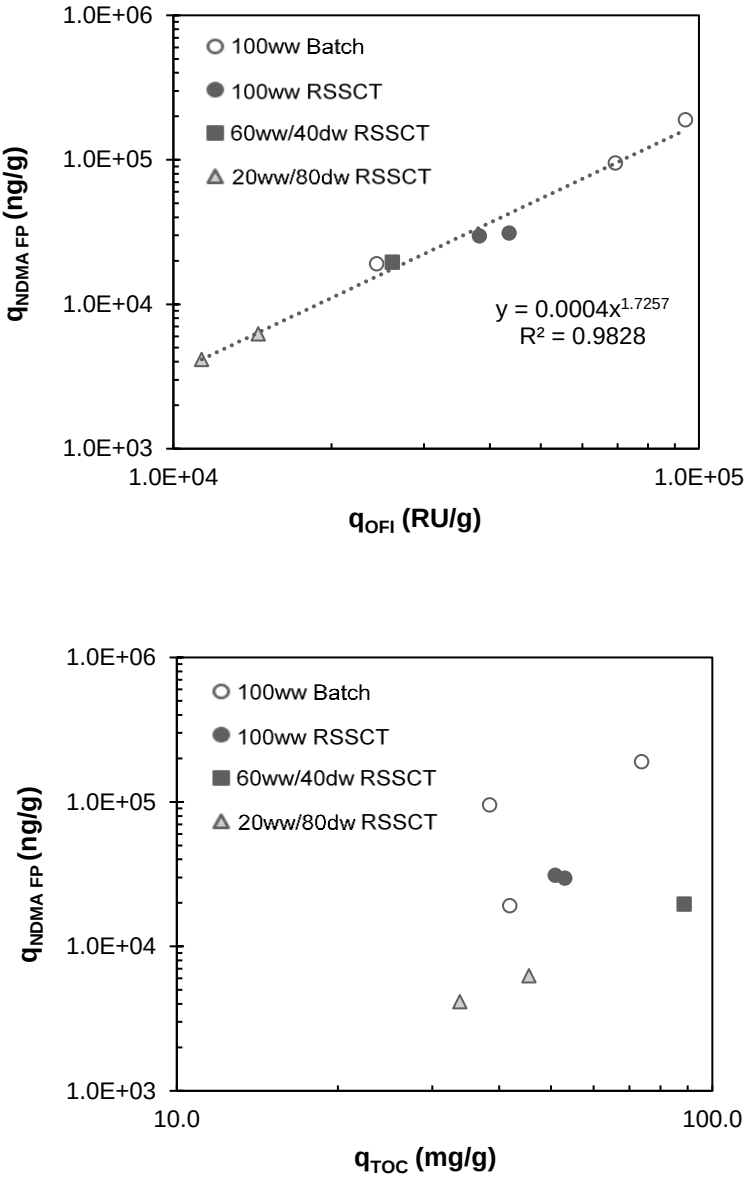

Figure 3.18: Correlation of GAC surface loading rates for OFI and TOC to NDMA FP.

Given the strength of this relationship, a nonlinear regression was also performed on normalized OFI breakthrough data in the same way as was done for NDMA FP in Figure 3.16. It is apparent in Figure 3.19 that normalized OFI data points also exhibit a consistent breakthrough behavior when considered as a single dataset. By correlating the two regression equations from

Figure 3.16 and Figure 3.19, a predictive model can be developed relating OFI breakthrough to NDMA FP breakthrough.

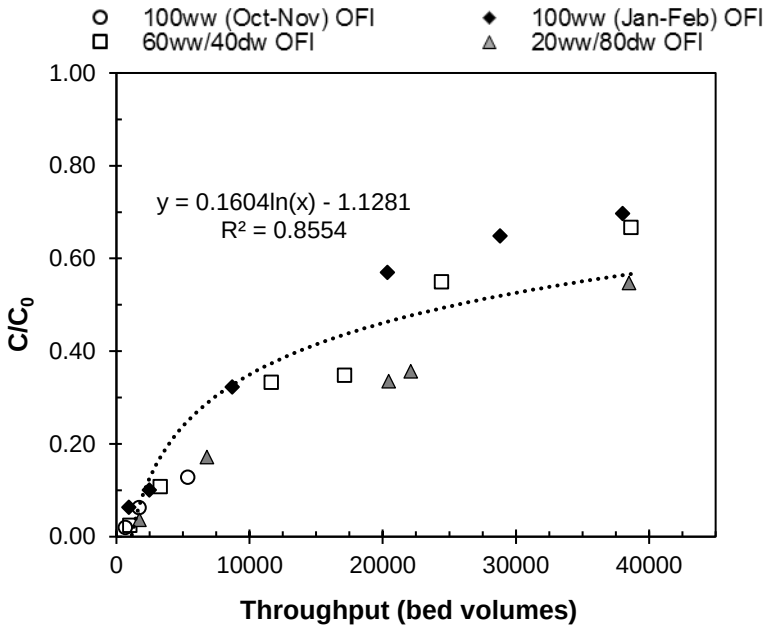

Figure 3.19: Normalized OFI breakthrough data considered together. Proposed model valid for TOC_0 = 2.2-6.1 mg/L and OFI_0 = 316-1438 RU.

Thus the following relationship is proposed for continuous-flow bench scale systems using lignite-based GAC:

$$\frac{[NDMA]}{[NDMA_0]} = 1.4196\frac{OFI}{OFI_0} - 0.2586 \qquad (4)$$

Equation 4 is valid in the range of influent conditions TOC_0 = 2.2-6.1 mg/L, NDMA FP_0 = 120-747 ng/L, and OFI_0 = 316-1438 R.U.

3.4.2 Effect of blending on chloraminated THM, HAA8, and HAN precursor removal

Chloraminated THM, HAA8, and HAN precursor removals also exhibited delayed breakthrough in waters with lower levels of background EfOM. These results are presented in Figure 3.14 and approximate values estimated for BV_{20} and BV_{50} are summarized in Table 3.5. With some exceptions, values in Table 3.5 increase by row from left to right, indicating that breakthrough for each compound occurs later as the wastewater effluent content decreases, and also increase by column from top to bottom, indicating which compounds generally breakthrough first and which breakthrough later. Chloraminated THM precursors are the first to break through in all four waters, passing through the column at approximately the same rate as TOC, especially in the first 5000 BV. This finding confirms that TOC functions well as an indicator of chloraminated THM precursor breakthrough, although UVA would be a more conservative surrogate. This is consistent with previous results in this study that found this relationship to be true in both 10 and 20 minute EBCTs.

Chloraminated HAN FP and HAA8 FP displayed similar breakthrough shapes as THM FP but with slightly better removal and correlated well to UVA breakthrough. Throughput to 50 percent breakthrough for THM FP ranged from approximately 2500 BV for 100ww to 15000 BV for 100dw, with the blended waters breaking through in between (Table 3.5). BV_{50} for HAN FP ranged from approximately 4500 BV for 100w to 17200 BV for 100dw, and HAA8 FP ranged from 3800 to 19700. Thus chloraminated HAN and HAA8 precursors break through to 50 percent in the column effluent 2000-5000 BV after THM precursors in all four waters. Overall, it is clear that none of the chloraminated carbonaceous DBP precursors exhibit sorption behavior like NDMA precursors and thus control of NDMA by GAC in wastewater effluent and drinking water needs to be considered separately from regulated DBPs.

3.4.3 Effect of source water on emerging DBP precursor removal

Monochloramine FP tests were performed on select effluent sample points from the 100ww (WW3) and 100dw (DW1) columns to understand the effects of GAC on additional emerging DBP precursors from wastewater effluent and drinking water sources. The complete list of emerging DBPs tested for at the University of South Carolina is provided in Appendix A1. In order to keep bromide levels constant, bromide was spiked in to DW1 to match the levels of WW3 (see Materials and Methods). The results of the FP testing on RSSCT breakthroughs are presented in Figure 3.20 and Figure 3.21.

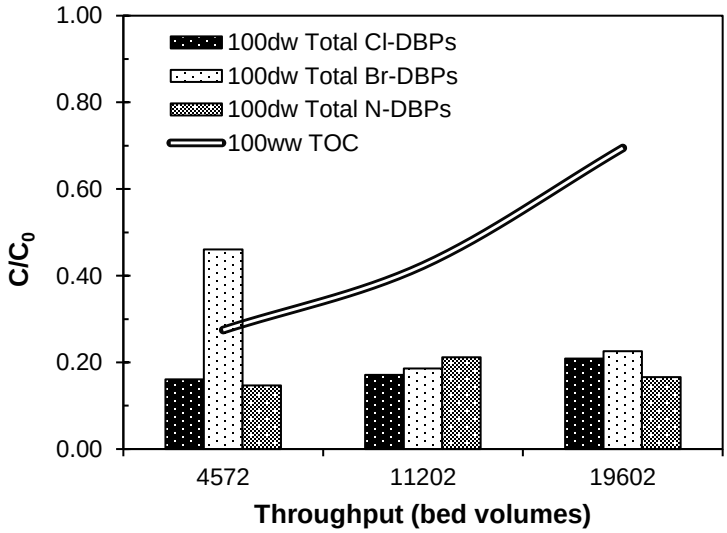

Figure 3.20: Breakthrough of emerging DBP precursors compared to TOC breakthrough for select sample points in the 100dw column. Raw water Total Cl-DBPs = 39.7 µg/L, Total Br-DBPs = 32.8 µg/L, Total I-DBPs = 0 µg/L, Total N-DBPs = 30.7 µg/L.

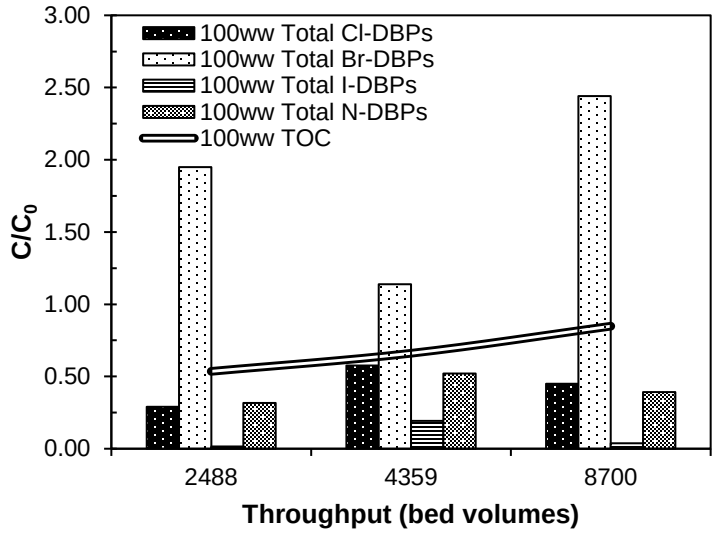

Figure 3.21: Breakthrough of emerging DBP precursors compared to TOC breakthrough for select sample points in the 100ww column. Raw water Total Cl-DBPs = 184.8 µg/L, Total Br-DBPs = 39.5 µg/L, Total I-DBPs = 5.74 µg/L, Total N-DBPs = 114.2 µg/L.

In DW1 no iodinated (I-DBPs) were formed at all. As can be seen in Figure 3.20, Total Nitrogenous DBPs (N-DBPs) and Chlorinated DBPs (Cl-DBPs) broke through the column slower than TOC overall, reaching only 20 percent breakthrough at approximately 20000 BV. High Total Brominated DBPs (Br-DBPs) were seen in the initial effluent of the DW1 column due to poor adsorbability of bromide, increasing the bromide to TOC ratio at early breakthrough points and consequently increasing relative Br-DBP formation. This shift toward brominated DBPs post-treatment has been explained by Summers et al. (1993) and others (Amy et al., 1995; Bougeard et al., 2010; Cowman and Singer, 1996). At later TOC breakthrough the influent bromide to TOC ratio appears to have returned and Total Br-DBPs concentrations drop in the chloraminated effluent.

As expected, WW3 saw greater absolute DBP formation for Total N-, Br-, I-, and Cl-DBPs. Total I-DBPs also saw low formation in the raw WW3 and in column effluents, while

Total Br-DBPs yielded more formation in the column effluents than influent (Figure 3.21). High Br-DBP values can also be attributed to the shift in bromide ion to organic matter ratio described above. In wastewater effluent, however, Total Br-DBPs increased, indicating poor adsorbability of wastewater-derived Br-DBP precursors compared to drinking-water precursors. Finally, Total N-DBPs and Cl-DBPs passed through the column slower than TOC, similar to the behavior of the drinking water column. N- and Cl- DBP WW3 precursors broke through the column much faster than DW1 precursors, reaching 39 and 44 percent breakthrough, respectively, as early as 8700 BV. Interestingly, Total N-DBPs in the wastewater column were not as effectively removed as NDMA specific precursors from the same column.

CHAPTER 4: CONCLUSIONS

4.1 Conclusions

The principal aims of this research were to a) understand the effects of disinfectant type and dose on DBP formation in wastewater effluent, with specific regard to NDMA, b) evaluate the effectiveness of GAC in removing NDMA formation potential relative to other wastewater-derived DBP precursors, c) provide insight to the effects of EBCT on wastewater effluent DBP precursor removal, and d) illuminate the effect of blending on adsorption behavior of wastewater-derived DBP precursors.

In regard to the above goals, NDMA formation was found to be greatest using monochloramine FP conditions in tertiary wastewater effluent. Chloraminated NDMA formation was greater in wastewater effluent than in drinking water, and found to result in greater formation with FP rather than UFC doses. Even using UFC doses, formation was higher than current EPA health goals. Wastewater-derived precursors formed higher concentrations of TTHMs and HAA8s using chlorine than monochloramine. TTHM and HAA8 formation were consistently higher than HAN and NDMA formation under both disinfectant types and doses.

In batch tests with four different PAC types, clear differences in NDMA FP removal were observed and correlated to carbon mesopore volumes, suggesting NDMA precursors in EfOM function in the mesopore size range in their sorption behavior. Overall, NDMA precursors seemed to adsorb independently of TOC and UVA and showed a non-adsorbable fraction of approximately 1 percent above a 10 mg/L PAC dose. Justification for considering NDMA precursors as trace organic constituents similar to micropollutants was proposed despite evidence

for heterogeneous precursor material. Other chloraminated DBP precursor removals paralleled OFI removal, while chlorinated DBP precursor removals were virtually identical to UVA and TOC removal. In addition, chloraminated DBP precursors were better removed by PAC than chlorinated DBP precursors in the batch tests, potentially due to selective adsorption of more aromatic, humic-like compounds that preferentially react with chloramines.

Initial RSSCTs testing two different EBCTs at the bench scale (10- and 20-minute simulated full-scale columns) revealed that NDMA FP was also better removed than TOC in the continuous-flow system. None of the chlorinated or chloraminated DBP precursors tested for exhibited similar breakthrough behavior to NDMA FP, providing further evidence of NDMA precursors distinct from EfOM. The 20-minute EBCT performed better than the 10-minute EBCT for TOC, UVA, and chloraminated DBP precursors, including NDMA. Chlorinated DBP precursors did not show as strong of a dependence on EBCT. Possible evidence of a fouling effect was seen to affect chloraminated DBP precursors and not chlorinated precursors.

Blending of RSSCT influent waters at ratios of 60ww/40dw and 20ww/80dw revealed that NDMA precursor sorption behavior follows a linear mass balance. Experimental NDMA FP breakthroughs matched with mass balance predicted breakthroughs. As a result, NDMA FP can be thought of as a conservative “tracer” of wastewater influence. It was found that TOC breaks through the column faster as the wastewater effluent content increases, due to faster exhaustion of the mass transfer zone with higher loading of EfOM. NDMA FP also generally follows this inverse relationship of increased breakthrough times with lower influent TOC, but not as strongly as TOC and UVA. Thus it was proposed that as a result of extremely low influent precursor concentrations linear isotherm effects may play a role in diminishing the effect of

influent concentration on breakthrough, a characteristic of trace organics/micropollutant sorption behavior.

RSSCT OFI breakthroughs were seen to follow similar linear mass balance behavior as NDMA FP with changing wastewater effluent content of the influent water. Correlating the surface loading of OFI to NDMA FP across all experiments (batch, blended and non-blended RSSCTs) revealed a precise power function relationship. Whether or not NDMA precursors are, in fact, also fluorophores is still unclear, but unlikely due to the non-linear correlation. Rather, evidence suggests that OFI is representative of more strongly adsorbing organic matter than TOC and thus has similar adsorbability to NDMA precursors. Regardless, this relationship was used as justification for developing a predictive model through linear and nonlinear regression analysis relating OFI removal to NDMA FP removal. The proposed model describes a general envelope for NDMA FP breakthrough within a specific set of influent conditions.

Finally, the effect of a shift toward brominated speciation of DBPs as a result of GAC treatment, as documented in the literature, was confirmed for wastewater effluent and drinking water. Whereas in drinking water the total brominated DBP concentration exhibited a return shift to less brominated DBPs by 50 percent TOC breakthrough, in the wastewater effluent column total brominated DBP levels remained higher in chloraminated effluent than the influent, even at 75 percent TOC breakthrough.

4.2 Further Research

The conclusions developed in this study are important steps toward controlling DBP precursors from wastewater effluent with GAC and, thereby, minimizing the public health impacts of wastewater reuse. However, in order to operationalize these findings at full-scale and

continue to make bench-scale tools for assessing GAC control of wastewater-derived precursors more useful, a comprehensive scale-up approach for the adsorption behavior of NDMA FP from these findings to pilot-scale columns is an ongoing research need. Additionally, a variety of wastewater effluents should be tested to evaluate reproducibility of results across water types, particularly regarding OFI and its ability to predict NDMA precursor removal. Finally, to better characterize the micropollutant behavior of NDMA precursors, additional RSSCTs run with diluted EfOM precursor material while maintaining constant TOC concentrations would provide conclusive evidence regarding influent precursor concentration independence during GAC treatment.

REFERENCES

Adler, R., Landman, J., Cameron, D., 1993. The Clean Water Act 20 Years Later. Island Press, Washington, D.C.

Amy, G., Siddiqui, M., Zhai, W., Debroux, J., Odem, W., 1995. Survey on bromide in drinking water and impacts on DBP formation.

APHA, 2005. Standard Methods for the Examination of Water and Wastewater, American Water Works Association/American Public Works Association/Water Environment Federation.

ATSDR, 1989. Toxicological Profile for N-Nitrosodimethylamine. Agency for Toxic Substances and Disease Registry (ATSDR), Atlanta, GA.

Barker, D.J., Stuckey, D.C., 1999. A review of soluble microbial products (SMP) in wastewater treatment systems. Water Res. 33, 3063–3082. doi:10.1016/S0043-1354(99)00022-6

Beggs, K.M.H., Summers, R.S., McKnight, D.M., 2009. Characterizing chlorine oxidation of dissolved organic matter and disinfection by-product formation with fluorescence spectroscopy and parallel factor analysis. J. Geophys. Res. Biogeosciences 114, 1–10. doi:10.1029/2009JG001009

Bell-Ajy, K., Abbaszadegan, M., Ibrahim, E., Verges, D., LeChevallier, M., 2000. Conventional and optimized coagulation for NOM removal. J. / Am. Water Work. Assoc. 92, 44–58.

Bond, R.G., Digiano, F.A., 2004. Evaluating GAC performance using the ICR Database. Am. Water Work. Assoc. 96, 96–104.

Bougeard, C.M.M., Goslan, E.H., Jefferson, B., Parsons, S.A., 2010. Comparison of the disinfection by-product formation potential of treated waters exposed to chlorine and monochloramine. Water Res. 44, 729–740. doi:10.1016/j.watres.2009.10.008

Buczek, B., 2016. Preparation of Active Carbon by Additional Activation with Potassium Hydroxide and Characterization of Their Properties. Adv. Mater. Sci. Eng. 2016, 1–4.

Cal/EPA, 2006. Public Health Goal for N-Nitrosodimethylamine in Drinking Water. California Enivironmental Protection Agency (Cal/EPA).

Chen, B., Westerhoff, P., 2010. Predicting disinfection by-product formation potential in water. Water Res. 44, 3755–3762. doi:10.1016/j.watres.2010.04.009

Choi, J., Valentine, R.L., 2002. Formation of N-nitrosodimethylamine (NDMA) from reaction of monochloramine: a new disinfection by-product. Water Res. 35, 817–824.

Clark, R.M., Adams, J.Q., Lykins, B.W.J., 1995. DBP control in drinking water: cost and performance. J. Environ. Eng. 120, 759–782.

Corwin, C.J., Summers, R.S., 2012. Controlling trace organic contaminants with GAC adsorption. J. Am. Water Works Assoc. 104, 43–44. doi:10.5942/jawwa.2012.104.0004

Corwin, C.J., Summers, R.S., 2010. Scaling trace organic contaminant adsorption capacity by granular activated carbon. Environ. Sci. Technol. 44, 5403–5408. doi:10.1021/es9037462

Cory, R.M., Miller, M.P., McKnight, D.M., Guerard, J.J., Miller, P.L., 2010. Effect of

instrument-specific response on the analysis of fulvic acid fluorescence spectra. Limnol. Oceanogr. Methods 8, 67–78. doi:10.4319/lom.2010.8.0067

Cowman, G.A., Singer, P.C., 1996. Effect of bromide ion on haloacetic acid speciation resulting from chlorination and chloramination of aquatic humic substances. Environ. Sci. Technol. 30, 16–24. doi:10.1021/es9406905

Crittenden, J., Berrigan, J., 1987. Design of rapid fixed-bed adsorption tests for nonconstant diffusivities. J. Environ. Eng. 113, 243–259. doi:10.1061/(ASCE)0733-9372(1987)113:2(243)

Crittenden, J.C., Sanjay Reddy, P., Arora, H., Trynoski, J., Hand, D.W., Perram, D.L., Summers, R.S., 1991. Predicting GAC Performance with Rapid Small-Scale Column Tests. Am. Water Work. Assoc. 83, 77–87.

Cutler, D., Miller, G., 2005. The Role of Public Health Improvements in Health Advances : The Twentieth-Century United States. Demography 42, 1–22.

Gilmore, P.L., Summers, R.S., 2015. Organic Matter Removal via Biological Drinking Water Filters: Removal Efficiency Based on Quantifiable System Factors, in: AWWA WQTC Conference Proceedings. American Water Works Association, Salt Lake City.

Goslan, E.H., Fearing, D.A., Banks, J., Wilson, D., Hills, P., Campbell, A.T., Parsons, S.A., 2002. Seasonal variations in the disinfection by-product precursor profile of a reservoir water. J. Water Supply Res. Technol. - AQUA 51, 475–482.

Graham, M.R., Summers, R.S., Simpson, M.R., MacLeod, B.W., 2000. Modeling equilibrium adsorption of 2-methylisoborneol and geosmin in natural waters. Water Res. 34, 2291–2300. doi:10.1016/S0043-1354(99)00390-5

Hanigan, D., Thurman, E.M., Ferrer, I., Zhao, Y., Andrews, S., Zhang, J., Herckes, P., Westerhoff, P., 2015. Methadone Contributes to N-nitrosodimethylamine Formation in Surface Waters and Wastewaters during Chloramination. Environ. Sci. Technol. Lett. 2, 151–157. doi:10.1021/acs.estlett.5b00096

Hanigan, D., Zhang, J., Herckes, P., Krasner, S.W., Chen, C., Westerhoff, P., 2012. Adsorption of N-nitrosodimethylamine precursors by powdered and granular activated carbon. Environ. Sci. Technol. 46, 12630–12639. doi:10.1021/es302922w

Holady, J.C., Trenholm, R.A., Snyder, S.A., 2012. Use of Automated Solid-Phase Extraction and GC-MS/MS to Evaluate Nitrosamines in Water Matrices. Am. Lab.

HSDB, 2013. N-Nitrosodimethylamine. U.S. National Library of Medicine Hazardous Substance Databank (HSDB).

Hua, G., Reckhow, D.A., 2007. Characterization of disinfection byproduct precursors based on hydrophobicity and molecular size. Environ. Sci. Technol. 41, 3309–3315. doi:10.1021/es062178c

Jacangelo, J.G., DeMarco, J., Owen, D.M., Randtke, S.J., 1995. Selected processes for removing NOM: An overview. J. / Am. Water Work. Assoc. 87, 64–77. doi:10.2307/41295153

Kilduff, J.E., Karanfil, T., Weber, W.J.J., 1998. Competitive Effects of Nondisplaceable Organic

Compounds on Trichloroethylene Uptake by Activated Carbon. II. Model Verification and Applicability to Natural Organic Matter. J. Colloid Interface Sci. 205, 280–289. doi:10.1006/jcis.1998.5603

Knappe, D.R.U., Matsui, Y., Snoeyink, V.L., Roche, P., Prados, M.J., Bourbigot, M.M., 1998. Predicting the capacity of powdered activated carbon for trace organic compounds in natural waters. Environ. Sci. Technol. 32, 1694–1698. doi:10.1021/es970833y

Kolpin, D.W., Furlong, E.T., Meyer, M.T., Thurman, E.M., Zaugg, S.D., Barber, L.B., Buxton, H.T., 2002. Pharmaceuticals, hormones, and other organic wastewater Contaminants in U.S. Streams, 1999-2000: A National Reconnaissance. Environ. Sci. Technol. 36, 1202–11. doi:10.1021/es011055j

Korak, J.A., Dotson, A.D., Summers, R.S., Rosario-Ortiz, F.L., 2014. Critical analysis of commonly used fluorescence metrics to characterize dissolved organic matter. Water Res. 49, 327–338. doi:10.1016/j.watres.2013.11.025

Korak, J.A., Rosario-Ortiz, F.L., Summers, R.S., 2014. Fluorescence Characterization of Humic Substance Coagulation : Application of New Tools to an Old Process.

Krasner, S.W., Lee, C.F.T., Liang, S., Mitch, W., Von Gunten, U., Westerhoff, P.K., 2012. Impact of a nitrified biofilter on NDMA formation, in: American Water Works Association Annual Conference and Exposition 2012, ACE 2012. Dallas, TX, pp. 3919–3943.

Krasner, S.W., McGuire, M.J., Jacangelo, J.G., Patania, N.L., Reagan, K.M., Marco Aieta, E., 1989. Occurrence of disinfection by-products in US drinking water. J. / Am. Water Work. Assoc. 81, 41–53. doi:10.2307/41292789

Krasner, S.W., Mitch, W. a., McCurry, D.L., Hanigan, D., Westerhoff, P., 2013. Formation, precursors, control, and occurrence of nitrosamines in drinking water: A review. Water Res. 47, 4433–4450. doi:10.1016/j.watres.2013.04.050

Krasner, S.W., Sclimenti, M.J., Mitch, W.A., Westerhoff, P., Dotson, A., 2007. Using formation potential tests to elucidate the reactivity of DBP precursors with chlorine versus with chloramines, in: American Water Works Association - Water Quality Technology Conference and Exposition 2007: Fast Tracks to Water Quality. Charlotte, NC, pp. 3184–3194.

Krasner, S.W., Westerhoff, P., Chen, B., Amy, G.L., Nam, S.-N., Chowdhury, Z.K., Sinha, S., Rittmann, B.E., 2008. Contribution of Wastewater to DBP Formation, AwwaRF Report.

Le Roux, J., Gallard, H., Croué, J.P., 2011. Chloramination of nitrogenous contaminants (pharmaceuticals and pesticides): NDMA and halogenated DBPs formation. Water Res. 45, 3164–3174. doi:10.1016/j.watres.2011.03.035

Li, C., 2011. Trends and Effects of Chloramine in Drinking Water. Water Cond. Purif. 53, 52–56.

Li, L., Quinlivan, P.A., Knappe, D.R.U., 2005. Predicting adsorption isotherms for aqueous organic micropollutants from activated carbon and pollutant properties. Environ. Sci. Technol. 39, 3393–3400. doi:10.1021/es048816d

Liang, L., Singer, P.C., 2003. Factors influencing the formation and relative distribution of haloacetic acids and trihalomethanes in drinking water. Environ. Sci. Technol. 37, 2920–2928. doi:10.1021/es026230q

Ma, H., Allen, H.E., Yin, Y., 2001. Characterization of Isolated Fractions of Dissolved Organic Matter From Natural Waters and a Wastewater Effluent. Wat. Res 35, 985–996.

Matsui, Y., Fukuda, Y., Inoue, T., Matsushita, T., 2003. Effect of natural organic matter on powdered activated carbon adsorption of trace contaminants: Characteristics and mechanism of competitive adsorption. Water Res. 37, 4413–4424. doi:10.1016/S0043-1354(03)00423-8

McKnight, D.M., Boyer, E.W., Westerhoff, P.K., Doran, P.T., Kulbe, T., Andersen, D.T., 2001. Spectrofluorometric characterization of dissolved organic matter for indication of precursor organic material and aromaticity. Limnol. Oceanogr. 46, 38–48. doi:10.4319/lo.2001.46.1.0038

Mezzari, I., 2006. Predicting the Adsorption Capacity of Activated Carbon for Organic Contaminants from Fundamental Adsorbent and Adsorbate Properties. North Carolina State University. doi:10.1017/CBO9781107415324.004

Mitch, W.A., Gerecke, A.C., Sedlak, D.L., 2003. A N-nitrosodimethylamine (NDMA) precursor analysis for chlorination of water and wastewater. Water Res. 37, 3733–3741.

Mitch, W.A., Sedlak, D.L., 2004. Characterization and Fate of N -Nitrosodimethylamine Precursors in Municipal Wastewater Treatment Plants. Environ. Sci. Technol. 38, 1445–1454. doi:10.1021/es035025n

Mitch, W.A., Sedlak, D.L., 2002. Formation of N-nitrosodimethylamine (NDMA) from dimethylamine during chlorination. Environ. Sci. Technol. 36, 588–595. doi:10.1021/es010684q

Mitch, W.A., Sharp, J.O., Trussell, R.R., 2003. N-nitrosodimethylamine (NDMA) as a drinking water contaminant: a review. Environ. Eng. Sci. 20, 389–404.

Mostafa, S., Korak, J.A., Shimabuku, K., Glover, C.M., Rosario-Ortiz, F.L., 2014. Relation between optical properties and formation of reactive intermediates from different size fractions of organic matter. ACS Symp. Ser. 1160, 159–179. doi:10.1021/bk-2014-1160.ch008

Pernet-coudrier, B., Clouzot, L., Varrault, G., Tusseau-vuillemin, M.H., Verger, A., Mouchel, J.M., 2008. Dissolved organic matter from treated effluent of a major wastewater treatment plant: Characterization and influence on copper toxicity. Chemosphere 73, 593–599. doi:10.1016/j.chemosphere.2008.05.064

Reddy, K.A., Doraiswany, L.K., 1967. Estimating Liquid Diffusivity. I&EC Fundam. 6, 77–79. doi:10.1021/i160021a012

Rice, J., Wutich, A., Westerhoff, P., 2013. Assessment of de facto wastewater reuse across the U.S.: Trends between 1980 and 2008. Environ. Sci. Technol. 47, 11099–11105. doi:10.1021/es402792s

Richardson, S.D., Plewa, M.J., Wagner, E.D., Schoeny, R., DeMarini, D.M., 2007. Occurrence, genotoxicity, and carcinogenicity of regulated and emerging disinfection by-products in drinking water: A review and roadmap for research. Mutat. Res. - Rev. Mutat. Res. 636, 178–242. doi:10.1016/j.mrrev.2007.09.001

Sedlak, D.L., Deeb, R.A., Hawley, E.L., Mitch, W.A., Timothy, D.D., Mowbray, S., Carr, S., 2005. Sources and Fate of Nitrosodimethylamine and Its Precursors in Municipal Wastewater Treatment Plants. Water Environ. Res. 77, 32–39.

Shen, R., Andrews, S. a., 2011. Demonstration of 20 pharmaceuticals and personal care products (PPCPs) as nitrosamine precursors during chloramine disinfection. Water Res. 45, 944–952. doi:10.1016/j.watres.2010.09.036

Shen, R., Andrews, S.A., 2013. NDMA formation from amine-based pharmaceuticals - Impact from prechlorination and water matrix. Water Res. 47, 2446–2457. doi:10.1016/j.watres.2013.02.017

Summers, R.S., Benz, M.A., Shukairy, H.M., Cummings, L., 1993. Effect of separation processes on the formation of brominated THMs. J. / Am. Water Work. Assoc. 85, 88–95.

Summers, R.S., Haist, B., Koehler, J., Ritz, J., Zimmer, G., Sontheimer, H., 1989. The influence of background organic matter on GAC adsorption. J. Am. Water Work. Assoc. 81, 66–74.

Summers, R.S., Hooper, S.M., Shukairy, H.M., Solarik, G., Owen, D., 1996. Assessing DBP yield: Uniform formation conditions. J. / Am. Water Work. Assoc. 88, 80–93.

Summers, R.S., Hooper, S.M., Solarik, G., Owen, D.M., Hong, S.H., 1995. Bench-Scale Evaluation of Gac for NOM Control. J. Am. Water Work. Assoc. 87, 69–80.

Summers, R.S., Kim, S.M., Shimabuku, K., Chae, S.H., Corwin, C.J., 2013. Granular activated carbon adsorption of MIB in the presence of dissolved organic matter. Water Res. 47, 3507–3513. doi:10.1016/j.watres.2013.03.054

Summers, R.S., Knappe, D.R.U., Snoeyink, V.L., 2010. Adsorption of Organic Compounds by Activated Carbon, in: Water Quality and Treatment: A Handbook on Drinking Water. American Water Works Association, McGraw-Hill, New York, NY.

USEPA, 2002. N-Nitrosodimethylamine. United States Enivironmental Protection Agency (USEPA) Integrated Risk Information System (IRIS).

Villanueva, C., Cantor, K., Cordier, S., Jaakkola, J., King, W., Lynch, C., Porru, S., Kogevinas, M., 2004. Disinfection byproducts and bladder cancer: a pooled analysis. Epidemiology 15, 357–367.

Waller, K., Swan, S., DeLorenze, G., Hopkins, B., 1998. Trihalomethanes in drinking water and spontaneous abortion. Epidemiology 9, 134–140.

Westerhoff, P., Yoon, Y., Snyder, S., Wert, E., 2005. Fate of endocrine-disruptor, pharmaceutical, and personal care product chemicals during simulated drinking water treatment processes. Environ. Sci. Technol. 39, 6649–6663. doi:10.1021/es0484799

Woods, G.C., Dickenson, E., 2015. Evaluation of the Final UCMR2 Database: Nationwide Trends in NDMA. Am. Water Work. Assoc. 107, 58–68.

Yoon, Y., Westerhoff, P., Snyder, S.A., Esparza, M., 2003. HPLC-fluorescence detection and adsorption of bisphenol A, 17??-estradiol, and 17??-ethynyl estradiol on powdered activated carbon. Water Res. 37, 3530–3537. doi:10.1016/S0043-1354(03)00239-2

Zachman, B.A., Rajagopalan, B., Summers, R.S., 2007. Modeling NOM Breakthrough in GAC Adsorbers Using Nonparametric Regression Techniques. Environ. Eng. Sci. 24, 1280–1296. doi:10.1089/ees.2006.0223

Zachman, B.A., Summers, R.S., 2010. Modeling TOC Breakthrough in Granular Activated Carbon Adsorbers. J. Environ. Eng. 136, 204–210. doi:10.1061/(ASCE)EE.1943-7870.0000145

Zhang, B., Xian, Q., Yang, G., Gong, T., Li, A., Feng, J., 2015. Formation potential of N-nitrosamines from soluble microbial products (SMPs) exposed to chlorine, chloramine and ozone. R. Soc. Chem. Adv. 5, 83682–83688. doi:10.1039/C5RA14631C

Zietzschmann, F., Muller, J., Sperlich, A., Ruhl, A.S., Meinel, F., Altmann, J., Jekel, M., 2014. Rapid small-scale column testing of granular activated carbon for organic micro-pollutant removal in treated domestic wastewater. Water Sci. Technol. 70, 1271–1278. doi:10.2166/wst.2014.357

APPENDIX

A1 Emerging DBP analytes

The following analytes were tested for at the University of South Carolina after monochloramine FP dosing on RSSCT influents and select effluents using 100 percent wastewater (WW3) and 100 percent drinking water (DW1).

TOTAL Cl-DBPs

Iodo-THMs
Dichloroiodomethane
Chlorodiiodomethane
Bromochloroiodomethane

Haloacetonitriles
Chloroacetonitrile
Dichloroacetonitrile
Bromochloroacetonitrile
Trichloroacetonitrile

Haloketones
Chloropropanone
1,1-Dichloropropanone
1,3-Dichloropropanone
1,1,1-Trichloropropanone
1,1,3-Trichloropropanone
1-Bromo-1,1-Dichloropropanone
1,1,3,3-Tetrachloropropanone

Haloaldehydes
Chloroacetaldehyde
Dichloroacetaldehyde
Bromochloroacetaldehyde
Trichloroacetaldehyde
Bromodichloroacetaldehyde
Dibromochloroacetaldehyde

Halonitromethanes
Dichloronitromethane
Bromochloronitromethane

TOTAL Br-DBPs

Iodo-THMs
Bromochloroiodomethane
Dibromoiodomethane
Bromodiiodomethane

Haloacetonitriles
Bromoacetonitrile
Bromochloroacetonitrile
Dibromoacetonitrile
Tribromoacetonitrile

Haloketones
1,1-Dibromopropanone
1-Bromo-1,1-Dichloropropanone
1,1,3,3-Tetrabromopropanone

Haloaldehydes
Bromoacetaldehyde
Bromochloroacetaldehyde
Dibromoacetaldehyde
Bromodichloroacetaldehyde
Dibromochloroacetaldehyde
Tribromoacetaldehyde

Halonitromethanes
Bromochloronitromethane
Dibromonitromethane
Dibromochloronitromethane
Tribromonitromethane (Bromopicrin)
Bromodichloronitromethane

Trichloronitromethane (Chloropicrin)
Dibromochloronitromethane
Bromodichloronitromethane

Haloamides
Chloroacetamide
Dichloroacetamide
Bromochloroacetamide
Trichloroacetamide
Bromodichloroacetamide
Dibromochloroacetamide
Chloriodoacetamide

Halobenzoquinones
2,6-Dichlorobenzoquinone
2,6-Dichloro-3-methylbenzoquinone
2,3,6-Trichlorobenzoquinone

Iodo-acids
Chloroiodoacetic acid

Haloamides
Bromoacetamide
Bromochloroacetamide
Dibromoacetamide
Bromodichloroacetamide
Dibromochloroacetamide
Tribromoacetamide
Bromoiodoacetamide

Halobenzoquinones
2,6-Dibromobenzoquinone

Iodo-acids
Bromoiodoacetic acid
(Z)-3-Bromo-3-iodo-propenoic acid
(E)-3-Bromo-3-iodo-propenoic acid

TOTAL I-DBPs

Iodo-THMs
Dichloroiodomethane
Chlorodiiodomethane
Bromochloroiodomethane
Dibromoiodomethane
Iodoform
Bromodiiodomethane

Haloacetonitriles
Iodoacetonitrile

Haloamides
Iodoacetamide
Chloriodoacetamide
Diiodoacetamide

Iodo-acids
Iodoacetic acid
Bromoiodoacetic acid
Diiodoacetic acid
Chloroiodoacetic acid

TOTAL N-DBPs

Haloacetonitriles
Chloroacetonitrile
Bromoacetonitrile
Dichloroacetonitrile
Bromochloroacetonitrile
Dibromoacetonitrile
Trichloroacetonitrile
Tribromoacetonitrile
Iodoacetonitrile

Halonitromethanes
Dichloronitromethane
Bromochloronitromethane
Dibromonitromethane
Trichloronitromethane (Chloropicrin)
Dibromochloronitromethane
Tribromonitromethane (Bromopicrin)
Bromodichloronitromethane

Haloamides
Chloroacetamide

(Z)-3-Bromo-3-iodo-propenoic acid	Bromoacetamide
(E)-3-Bromo-3-iodo-propenoic acid	Dichloroacetamide
	Bromochloroacetamide
	Dibromoacetamide
	Trichloroacetamide
	Bromodichloroacetamide
	Dibromochloroacetamide
	Tribromoacetamide
	Bromoiodoacetamide
	Iodoacetamide
	Chloriodoacetamide
	Diiodoacetamide

A2 Emerging DBP sampling and extraction methods

The following sampling and extraction methods for emerging DBP analysis were provided from the research group of Dr. Susan D. Richardson in the Department of Chemistry and Biochemistry at the University of South Carolina.

A2.1 Sampling Methods

No quenching was required for chloramination FP testing. Samples were shipped in 1 L glass amber bottles with no headspace. Sulfuric acid was added for preservation and to avoid base hydrolysis of some compounds.

A2.2 Extraction Methods

Iodo-trihalomethanes (I-THMs), haloacetonitriles (HANs), haloketones (HK), tri-haloaldehydes (HAls), halonitromethanes (HNMs), and haloamides (HAms) were extracted at a pH between 3-5, using a standard liquid-liquid extraction technique with methyl tert-butyl ether (MTBE) as a solvent. 30 grams of sodium sulfate were added to provide a salting-out effect and increases extraction recoveries.

HANs, HAms, along with tribromoacetonitrile (TBAN), tribromonitromethane, dibromochloronitromethane (DBCNM), bromodichloronitromethane (BDCNM), and tribromonitromethane (TBNM) were extracted at pH < 1 using 3 separate aliquots of MTBE, which were placed into one test tube and concentrated under nitrogen. The extract was separated into two vials and one vial was derivatized using a diazomethane derivatization procedure in order to quantify the iodo-acids (I-HAAs). It has been reported that haloamides are most stable at pH 3-5 and are susceptible to base hydrolysis as well, so there was concern that these

compounds would degrade at a pH < 1. Since extraction is conducted immediately after pH adjustment, degradation of HAms was not observed and detection limits were seemingly unaffected. TBAN, DBCNM, BDCNM and TBNM were calibrated using a separated calibration curve because a reaction occurs with some iodinated compounds and affects the detection limits for iodinated HAms and I-HAAs.

Mono,di-aldehydes were first derivatized with an O-(2,3,4,5,6-pentafluorobenzyl)hydroxylamine (PFBHA) derivatization method and then extracted with multiple aliquots of hexane.

A3 Biological removal of wastewater-derived NDMA precursors

A3.1 Method

In order to understand the possible of effects of biological degradation of NDMA precursors in the RSSCT columns, a single-pass biologically active filtration experiment was run in accordance with procedures developed by Gilmore and Summers (2015).

WW3 was used in a bench scale system. Columns were run at a flow rate of 8.1 mL/min and a hydraulic loading rate of 4.6 mL/min/cm^2. The test was run twice using inert anthracite media, and biologically activated carbon (BAC) from CCWRD in order to distinguish the removal effects of biodegradation and adsorption versus biodegradation alone. Each media was allowed to acclimate to the water by recirculating 4 liters for 4 hours before the single-pass test was run. Effluent samples were taken at two different empty bed contact times (EBCTs) of 7.5 and 20 minutes and, after filtering through a 1.1 µm glass filter, were tested for DOC and NDMA FP.

A3.2 Results

Both media types and EBCTs showed removal of NDMA FP, and both showed that the longer EBCT also achieved better removal. The BAC was significantly more effective at removing NDMA FP, achieving 71 percent and 88 percent removal for the 7.5 and 20 minute EBCTs, respectively, while the anthracite column only showed 5 percent and 12 percent removals (Figure A3.1). This is likely due to the adsorption capacity still available to the BAC column due to biological regeneration, while the anthracite column shows biological degradation alone. It is unknown whether or not the biological degradation process adds some fraction of precursor load to the effluent, but it is clear that biologically active treatment is capable of

achieving an overall net removal of NDMA FP. Overall, it is clear that the potential to remove NDMA precursors using biologically active adsorptive media far exceeds that of the inert media and biodegradation alone.

DOC removals follow the same trend of performance between anthracite and BAC and the two EBCTs, with BAC and the 20 minute EBCT performing better in all cases, although removal is less pronounced than NDMA FP (Figure A3.2). This is likely due to the fact that the CCWRD water has already passed through a biologically active filtration process during the full-scale treatment train, so the remaining effluent organic matter is not readily biodegradable.

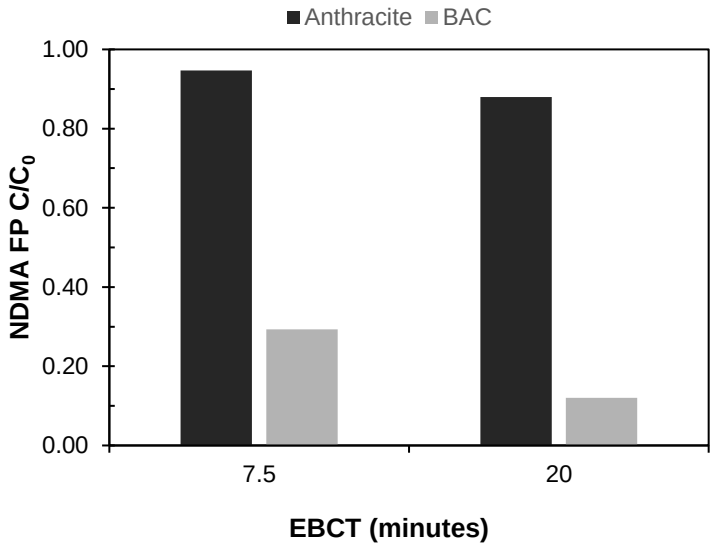

Figure A3.1: Fractional NDMA FP removal for anthracite and BAC at two different EBCTs. Raw water NDMA FP = 747 ng/L

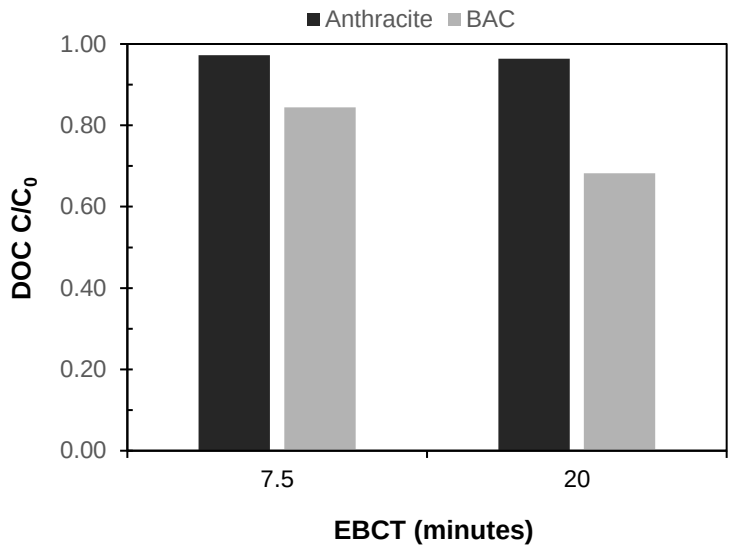

Figure A3.2: Fractional DOC removal for anthracite and BAC columns at two different EBCTs. Raw water DOC = 6.1 mg/L